

Theoretical guarantees for neural estimators in parametric statistics

Almut Rödder¹, Manuel Hentschel², and Sebastian Engelke²

¹ETH Zürich

²University of Geneva

Abstract

Neural estimators are simulation-based estimators for the parameters of a family of statistical models, which build a direct mapping from the sample to the parameter vector. They benefit from the versatility of available network architectures and efficient training methods developed in the field of deep learning. Neural estimators are amortized in the sense that, once trained, they can be applied to any new data set with almost no computational cost. While many papers have shown very good performance of these methods in simulation studies and real-world applications, so far no statistical guarantees are available to support these observations theoretically. In this work, we study the risk of neural estimators by decomposing it into several terms that can be analyzed separately. We formulate easy-to-check assumptions ensuring that each term converges to zero, and we verify them for popular applications of neural estimators. Our results provide a general recipe to derive theoretical guarantees also for broader classes of architectures and estimation problems.

1 Introduction

Estimation of the parameters of a family of distributions $\{\mathcal{P}_\theta\}_{\theta \in \Theta}$, taking values in $\mathcal{Z} \subseteq \mathbb{R}^d$ and parametrized by $\theta \in \Theta \subseteq \mathbb{R}^p$, is one of the most classical problems in statistics. The two main approaches are frequentist maximum-likelihood estimators and Bayes estimators relying on posterior distributions. In both settings we can define the set of all point estimators as $\mathcal{F} = \{f : \mathcal{Z}^m \rightarrow \mathbb{R}^p\}$ that map m i.i.d. samples $Z = (Z^1, \dots, Z^m)$ from some \mathcal{P}_θ to an estimate $\hat{\theta}$. The asymptotic properties of such estimators is well-understood [van der Vaart, 1998].

In many modern applications, the likelihood function is not available, or its evaluation is computationally prohibitive. This includes examples in cosmology [Alsing et al., 2019], spatial Gaussian random fields [Rue and Held, 2005] or max-stable distributions [de Haan, 1984]. In some cases, composite likelihood approaches are a computationally faster alternative, but may result in significant efficiency loss [Varin et al., 2011]. Simulation from such models is typically possible and computationally relatively cheap. For this reason, different simulation-based (or likelihood-free) inference methods have been developed, including indirect inference [Gourieroux et al., 1993] and the well-known approach of approximate Bayesian computation (ABC) [Beaumont et al., 2002]. Designing informative summary statistics can however be difficult and bad choices may lead to suboptimal performance.

Similar to ABC, neural estimators are simulation-based methods in the Bayesian setting. For a given loss function ℓ , the Bayes estimator f_m^* minimizes the weighted risk

$$R(f) = \int_{\Theta} \mathbb{E}_\theta [\ell(f(Z), \theta)] \pi(\theta) d\theta, \quad (1)$$

over all estimators $f \in \mathcal{F}$, where the weight function $\pi(\theta)$ is the density of the prior distribution on Θ [e.g., van der Vaart, 1998]. The corresponding Bayes risk $R(f_m^*)$ is thus the smallest possible population error for sample size m . We focus here on the quadratic loss $\ell(\hat{\theta}, \theta) = \|\hat{\theta} - \theta\|_2^2$ where the Bayes estimator is given by the conditional expectation $f_m^*(z) = \mathbb{E}(\theta \mid Z = z)$, $z \in \mathcal{Z}^m$. With this perspective of an estimator as a function from data to parameters, neural networks are a natural candidate to learn this function in light of the universal approximation property [Cybenko, 1989].

A neural estimator frames parameter estimation as supervised learning problem with the following steps. We first generate the training data consisting of N samples $\theta_1, \dots, \theta_N$ from the prior distribution $\pi(\theta)$ and consider one sample $Z_i = (Z_i^1, \dots, Z_i^m) \in \mathcal{Z}^m$ from $\mathcal{P}_{\theta_i}^m$ for each of them, $i = 1, \dots, N$. The pair (Z_i, θ_i) can be seen as an independent draw of a predictor-response pair of the training distribution in a prediction problem. The neural estimator is then the minimizer of the empirical version $R_N(f)$ of the population risk in (1) based on this simulated data set, i.e., the empirical risk minimizer

$$\phi_m^N = \arg \min_{\phi \in \Phi} \frac{1}{N} \sum_{i=1}^N \|f_\phi(Z_i) - \theta_i\|_2^2, \quad (2)$$

where we optimize over all neural networks $f_\phi : \mathcal{Z}^m \rightarrow \mathbb{R}^p$ parametrized by the set Φ of all considered network parameters, architectures and activation functions. Figure 1 illustrates the architecture of a neural estimator with a fully connected neural network; we will use the parameter ϕ and its induced neural network f_ϕ exchangeably. In practice, it is typically not possible and not desired to obtain the global minimizer ϕ_m^N exactly. Instead, regularization methods such as penalties, dropout and early stopping are employed during training to avoid overfitting [Goodfellow et al., 2016]. The resulting estimator $\hat{\phi}_m^N$ usually has a larger training risk (2) but a smaller population risk (1).

The fundamental difference of neural estimators to classical simulation-based approaches such as ABC is that they are amortized, that is, the only significant computational cost is at training time. Once the neural estimator is trained, it can be applied to any new data set

with m samples from \mathcal{P}_θ for an arbitrary $\theta \in \Theta$ essentially for free, since the forward pass in a neural network is computationally very cheap. Moreover, unlike ABC, neural Bayes estimators do not rely on fixed summary statistics but directly build a map from the data set to the parameter. Intuitively, the summary statistics are learned automatically as latent representations of the network.

The concept of neural estimators exists since a long time and they have been applied to various problems such as parameter estimation in times series [Chon and Cohen, 1997] and birth-and-death processes [Bokma, 2006] using dense networks. More recently, different architectures such as convolutional layers for efficient inference in temporal [Rudi et al., 2022] or spatial observations [Gerber and Nychka, 2021, Lenzi et al., 2021, Walchessen et al., 2024] or deep sets for multiple replicates [Sainsbury-Dale et al., 2023] have been proposed. While these methods seem to work well in practice and allow for very fast inference, so far no theoretical guarantees for the asymptotic or pre-asymptotic behavior of neural estimators exist; see, for instance, the discussion in Zammit-Mangion et al. [2025].

Our contribution is threefold. We first decompose the population risk $R(\tilde{\phi}_m^N)$ of the fitted neural estimator with m replicates and based on N simulated training data as

$$R(\tilde{\phi}_m^N) = \underbrace{R(f_m^*)}_{\text{Bayes Risk}} + \underbrace{R(\phi_m^*) - R(f_m^*)}_{\text{Approximation Error}} + \underbrace{R(\phi_m^N) - R(\phi_m^*)}_{\text{Generalization Error}} + \underbrace{R(\tilde{\phi}_m^N) - R(\phi_m^N)}_{\Delta \text{Algorithm}}; \quad (3)$$

see Figure 2 for a geometric illustration of this decomposition. The risk of a neural estimator therefore differs from the optimal Bayes risk through three error terms: the approximation error quantifies how well the class of neural networks Φ can approximate the Bayes estimator; the generalization error measures the amount of overfitting of the empirical risk minimizer ϕ_m^N compared to the optimal neural network estimator; and a term that depends on the optimization algorithm and regularization scheme used during training. This last term is typically negative due to the positive effect of regularization on the generalization of the network. We do not consider it here and refer to the literature on numerical analysis and statistical learning theory for details [e.g., Xing et al., 2018, and references therein]. We study all other terms of decomposition (3) separately and formulate easy-to-check assumptions under which they converge to zero as $m, N \rightarrow \infty$. This involves results from different fields such as the approximation theory of neural networks [Cybenko, 1989], robustness [Xu and Mannor, 2012], and statistical efficiency of Bayes estimators [van der Vaart, 1998]. Combining the results, we show consistency of neural estimators ϕ_m^N in a Bayesian sense. We further discuss that this estimator can be fully efficient compared to the Bayes estimator f_m^* under certain conditions.

As a second contribution, we check the assumptions of our theory for some of the most common applications of neural estimators. For spatial Gaussian processes with many locations, for instance, likelihood estimation can become prohibitively expensive [Rue and Held, 2005], but simulation remains feasible. For multivariate max-stable distributions in extreme value theory, full-likelihood inference becomes infeasible even in moderate dimensions [Wadsworth, 2015, Dombry et al., 2017b], but simulation can be done efficiently [Dombry et al., 2016].

Thirdly, our work provides a clear guide for proving asymptotic properties of neural estimators also in other settings. The error decomposition (3) separates the overall task into sub-problems from different disciplines and allows focussing on the relevant terms. For instance, if a different network architecture is used (e.g., convolutional or graph neural networks) for the same parametric family \mathcal{P}_θ , the Bayes risk will not be affected, and only the risk terms related to neural networks architectures change. On the other hand, for a different parametric model class, only the Bayes risk and a small condition on the tail heaviness of the statistical model $Z \sim \mathcal{P}_\theta$ have to be studied if the network architecture and training procedure remains the same.

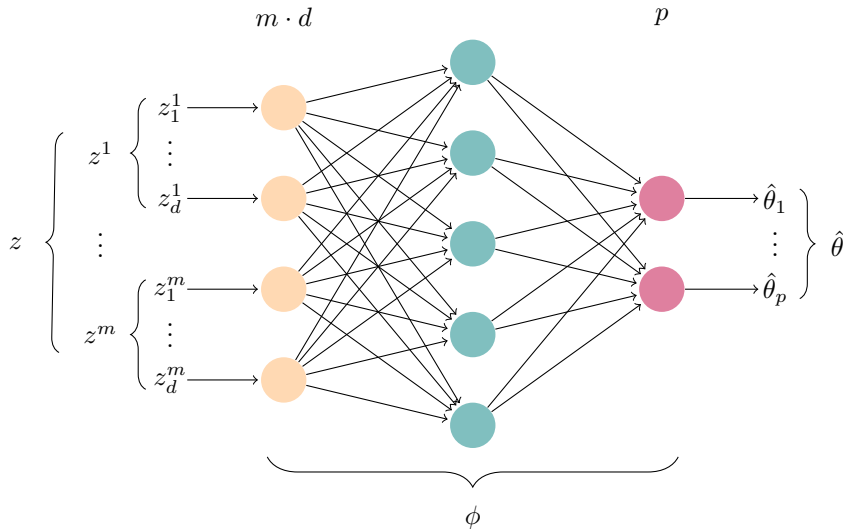


Figure 1: Example of a fully-connected neural network used as a neural estimator $f_\phi : \mathcal{Z}^m \rightarrow \mathbb{R}^p$. The size of the input and output layer is indicated above. Note that the subscripts to each z^i and θ indicate the corresponding dimension in the input and output space, whereas in the rest of this paper, they denote the index $1, \dots, N$ of each sequential training sample.

2 Setup and risk decomposition

We introduce the mathematical notation more formally in Section 2.1 and present the error decomposition in Section 2.2. Section 2.3 discusses Gaussian random field models and max-stable distributions, which serve as running examples used to illustrate our results throughout the paper.

2.1 Setup and notation

We consider a family of distributions, $\{\mathcal{P}_\theta\}_{\theta \in \Theta}$, taking values in $\mathcal{Z} \subseteq \mathbb{R}^d$ and parametrized by $\theta \in \Theta \subseteq \mathbb{R}^p$, for some $d, p \in \mathbb{N}$. The goal is to estimate the parameter θ from m i.i.d. samples $Z = (Z^1, \dots, Z^m)$, taking values in $\mathcal{Z}^m \subseteq \mathbb{R}^D$, for $D = md$, with $Z^i \sim \mathcal{P}_\theta$, or equivalently $Z \sim \mathcal{P}_\theta^m$. Throughout this paper, we consider a continuous distribution with respect to the Lebesgue measure, having density $p_\theta : \mathbb{R}^d \rightarrow \mathbb{R}$ (set to zero outside \mathcal{Z}). The joint density of Z is then given by

$$p_{\theta,m}(z) = \prod_{i=1}^m p_\theta(z^i), \quad z \in \mathbb{R}^D.$$

For a true parameter θ , the quality of an estimate $\hat{\theta}$ is quantified by the loss function ℓ . Note that we allow the estimate to be from \mathbb{R}^p , since a general estimator might map to values outside Θ . In general, there are few restrictions on the loss function, but we will mostly consider the quadratic loss

$$\begin{aligned} \ell : \mathbb{R}^p \times \Theta &\longrightarrow \mathbb{R} \\ (\hat{\theta}, \theta) &\longmapsto \ell(\hat{\theta}, \theta) = \|\hat{\theta} - \theta\|_2^2. \end{aligned} \quad (4)$$

Let \mathcal{F} denote the set of measurable functions from \mathcal{Z}^m to \mathbb{R}^p . To quantify the quality of an estimator $f \in \mathcal{F}$, for a given true parameter θ , we consider the point-wise risk

$$R_\theta(f) = \mathbb{E}_{Z \sim \mathcal{P}_\theta^m} \ell(f(Z), \theta) = \int_{\mathcal{Z}^m} p_{\theta,m}(z) \|f(z) - \theta\|_2^2 dz,$$

assuming a density and the quadratic loss function in the second equality. For a cleaner notation, the number of simultaneous samples m is implied by the domain of f , and not denoted explicitly.

In the Bayesian setting, which is implicitly assumed here, the parameter θ is considered to be a random variable distributed according to a prior distribution Π , which is typically absolutely continuous with respect to the Lebesgue measure with density $\pi : \Theta \rightarrow \mathbb{R}$. The quality of an estimator f is then quantified by the risk

$$R(f) = \mathbb{E}_{\theta \sim \Pi} R_\theta(f) = \int_{\Theta} \int_{\mathcal{Z}^m} \pi(\theta) p_{\theta, m}(z) \|f(z) - \theta\|_2^2 dz d\theta,$$

again assuming densities and the quadratic loss function in the second equality; see also (1). An estimator f_m^* that minimizes the risk R for m samples is called a Bayes estimator and the corresponding risk $R(f_m^*)$ is called the Bayes risk. For the quadratic loss function, the Bayes estimator is given by the conditional expectation $f_m^*(z) = \mathbb{E}(\theta | Z = z)$, $z \in \mathcal{Z}^m$. In the following, unless stated otherwise, we assume that both Π and \mathcal{P}_θ are continuous, having Lebesgue densities π and p_θ , and consider the quadratic loss function from (4).

Since the population risk $R(f)$ of some estimator $f \in \mathcal{F}$ is not accessible, it is typically approximated by the empirical risk. To this end, let $N \in \mathbb{N}$ be the number of samples $\theta_1, \dots, \theta_N$ from $\theta \sim \Pi$, and consider one sample from \mathcal{P}_θ^m for each of them, denoted by $Z_i = (Z_i^1, \dots, Z_i^m) \in \mathcal{Z}^m$, for $i = 1, \dots, N$. In general, we could also consider multiple samples per θ . The empirical version of $R(f)$ is then given by

$$R_N(f) = \frac{1}{N} \sum_{i=1}^N \ell(f(Z_i), \theta_i) = \frac{1}{N} \sum_{i=1}^N \|f(Z_i) - \theta_i\|_2^2,$$

where, as above, we assume the quadratic loss function in the second equation. Note that empirical risks are random variables, since they depend on the random samples Z_i and θ_i .

In the context of neural estimators, the function $f : \mathcal{Z}^m \rightarrow \mathbb{R}^p$ is given by a neural network. For a given input size m , architecture and activation function, a neural network with L layers is parametrized by its weight matrices $\{w^{(l)}\}_{l=1, \dots, L}$ and bias vectors $\{\beta^{(l)}\}_{l=1, \dots, L}$, collectively denoted as $\phi_m = (w, \beta)$, or just ϕ when the input size is implied. For a given parameter vector ϕ we denote by f_ϕ the corresponding map from \mathcal{Z}^m to \mathbb{R}^p . Below, the corresponding risks are abbreviated as $R(\phi) := R(f_\phi)$ and $R_N(\phi) := R_N(f_\phi)$.

A full list of symbols used in this paper can be found in Appendix D.

2.2 Error decomposition

For the sake of a clearer exposure, we assume in the following that all minimizers exist and are unique. This assumption does not fundamentally restrict the presented decompositions. Indeed, existence could be guaranteed by considering compact parameter spaces for neural networks, and in the case of non-unique minimizers, one could be chosen arbitrarily. On the other hand, the error decomposition in (6) could also be rephrased by considering the infimum of the risks, $\inf_{\phi \in \Phi} R(\phi)$, rather than the risk of the minimizer $R(\phi_m^*)$.

Recall that all expressions containing N , either as a subscript to the risk or as a superscript to the parametrization, are random variables, since they depend on the training data set. As discussed in the introduction, the Bayes estimator $f_m^* = \arg \min_{f \in \mathcal{F}} R(f)$ can be approximated by a neural network $f_{\phi_m^*}$ satisfying

$$\phi_m^* = \arg \min_{\phi \in \Phi} R(f_\phi), \tag{5}$$

where Φ denotes the set of all considered network parameters, architectures, and activation functions. There is a huge literature on possible architectures of neural networks. A concrete example of the parametrization Φ are single-layer, fully-connected neural networks.

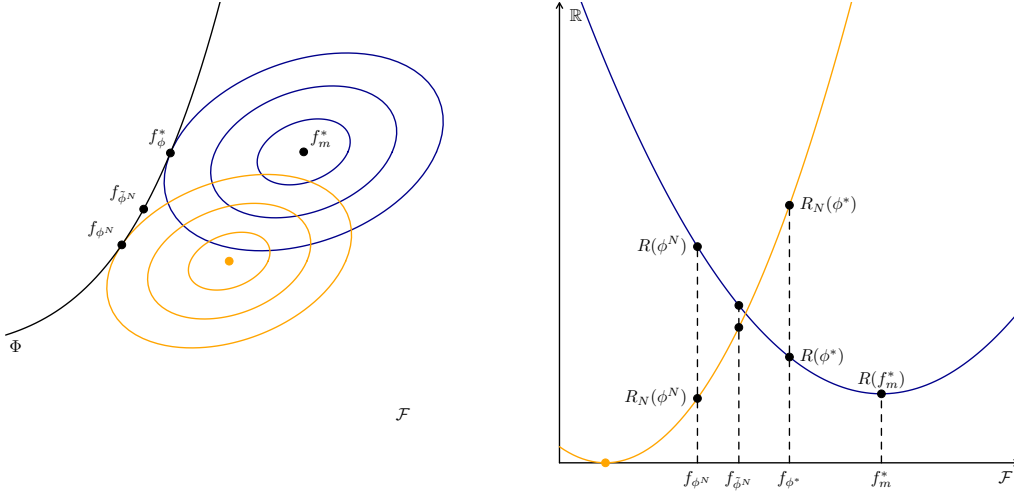


Figure 2: Schematic illustration of the different estimators and risks in the decompositions (6) and (7). Left: The coordinate system represents the space \mathcal{F} of all possible estimators, and the black line the subset that are neural networks Φ . The blue contour lines correspond to the population risk R , its minimizer in \mathcal{F} is the Bayes estimator f_m^* , and in Φ is $f_{\phi_m^*}$. The orange contour lines correspond to the empirical risk R_N , its minimizer over \mathcal{F} is usually zero, e.g., achieved by a 1-nearest neighbor estimator. Right: The x-axis is a slice of \mathcal{F} , and the blue and orange curves represent the population risk and empirical risk, respectively.

Example 2.1. Consider the family of single-layer, fully-connected, feedforward neural networks with D input neurons, N_1 hidden neurons, and a single output neuron, with activation function σ applied to the hidden neurons. This set can be denoted as

$$\Phi = \{\phi = (w, \beta) \mid w^{(1)} \in \mathbb{R}^{N_1 \times D}, w^{(2)} \in \mathbb{R}^{1 \times N_1}, \beta^{(1)} \in \mathbb{R}^{N_1}, \beta^{(2)} \in \mathbb{R}\},$$

where $w^{(1)}$ and $w^{(2)}$ are the weight matrices, and $\beta^{(1)}$ and $\beta^{(2)}$ are the bias vectors. The corresponding set of functions contains all neural networks of the form

$$f_\phi(z) = \beta^{(2)} + \sum_{j=1}^{N_1} w_j^{(2)} \sigma(w_j^{(1)} z + \beta_j^{(1)}), \quad z \in \mathbb{R}^D.$$

Since the population risk R in (5) is a theoretical quantity, we instead need to consider the empirical risk minimizer

$$\phi_m^N = \arg \min_{\phi \in \Phi} R_N(f_\phi).$$

In practice, yet another network, denoted $\tilde{\phi}_m^N$, is trained, due to several reasons. First, the optimization problem (5) is non-convex, and usually infeasible to solve exactly. Second, and more importantly, it is well-known that considering the naive empirical risk minimizer leads to overfitting, which can be mitigated by regularization techniques. These differences are illustrated and discussed in a simulation study in Section 7; for the theoretical results in the following sections, we will focus on ϕ_m^N .

Using the above chain of approximations ($f_m^* \approx f_{\phi_m^*} \approx f_{\phi_m^N}$), the population risk $R(\phi_m^N)$ of the empirical risk minimizer can be decomposed as

$$R(\phi_m^N) = \underbrace{R(f_m^*)}_{\text{Bayes Risk}} + \underbrace{R(\phi_m^*) - R(f_m^*)}_{\text{Approximation Error}} + \underbrace{R(\phi_m^N) - R(\phi_m^*)}_{\text{Generalization Error}}. \quad (6)$$

The first term is the Bayes risk, inherent to the task of predicting parameters of a distribution based on a finite number of observations $Z = (Z^1, \dots, Z^m)$. The second term is the error incurred by approximating the Bayes estimator $f_m^*(z) = \mathbb{E}(\theta|Z = z)$ with a neural network $f_{\phi_m^*}$, considering an optimal parametrization ϕ_m^* (with respect to a suitable choice of architecture and activation function, discussed in Section 4).

The third term, the generalization error, is due to using the parameters ϕ_m^N , learned from N training samples, rather than the optimal ϕ_m^* . It can be further decomposed into

$$\underbrace{R(\phi_m^N) - R(\phi_m^*)}_{\text{Generalization Error}} = \underbrace{R(\phi_m^N) - R_N(\phi_m^N)}_{\text{Generalization Error 2}} + \underbrace{R_N(\phi_m^N) - R_N(\phi_m^*)}_{\leq 0 \text{ a.s.}} + \underbrace{R_N(\phi_m^*) - R(\phi_m^*)}_{\rightarrow 0}, \quad (7)$$

which is driven by the first term, $R(\phi_m^N) - R_N(\phi_m^N)$, i.e., the discrepancy between the true risk R and the empirical risk R_N used to find ϕ_m^N . The last two terms are easy to control with conventional techniques. Indeed, the second term is non-positive, since ϕ_m^N is optimal with respect to the empirical risk R_N , and the third term converges to zero, because $R_N(\phi_m^*)$ is a finite sample approximation of $R(\phi_m^*)$.

Figure 2 shows a schematic illustration of the estimators and risks appearing in the decompositions (6) and (7), also including the regularized version $\tilde{\phi}_m^N$ of ϕ_m^N .

2.3 Examples

Before presenting the main theoretical results, we introduce several models that are commonly used in the literature of neural estimators. Throughout the paper, we will verify the main assumptions on these examples to show the broad applicability of our results.

Neural estimators are particularly useful in settings where the likelihood function is intractable but simulation from the model is possible. A typical example of this is parameter estimation in for spatial or spatio-temporal Gaussian random field models, where likelihood inference becomes computationally infeasible in higher dimensions [Gerber and Nychka, 2021, Sainsbury-Dale et al., 2023]. Another popular example are max-stable distributions de Haan [1984] or max-stable random fields [Lenzi et al., 2021], where evaluation of the full likelihood is impossible already in moderate dimensions [Dombry et al., 2017b], but exact simulation is feasible [Dombry et al., 2016].

In Appendix C we discuss the illustrative example of estimation of the parameters of a linear model. Since in this case we have more explicit representations of risk terms in the decomposition (6), it provides intuition on the different error contributions in neural estimation.

2.3.1 Gaussian random fields

A Gaussian random field is a stochastic process $W = \{W(s) : s \in S\}$ on some domain $S \subseteq \mathbb{R}^k$ such that for any finite set of points $s_1, \dots, s_d \in S$, the random vector $(W(s_1), \dots, W(s_d))$ follows a multivariate normal distribution. Without losing generality, we restrict the model to have a known constant mean zero, and we consider stationary, isotropic covariance function. The distribution is then fully characterized by the covariance function $\text{Cov}(W(s), W(s')) = C(\|s - s'\|)$. Neural estimators are parametric methods, and we therefore consider a parametric family consisting of a continuous covariance function $\tilde{C}_{\tilde{\theta}}(h)$ with nugget effect $\tau^2 \mathbb{1}_{h=0}$, that is,

$$C_{\theta}(h) = \tilde{C}_{\tilde{\theta}}(h) + \tau^2 \mathbb{1}_{h=0}.$$

This model is parametrized by $\theta = (\tau, \tilde{\theta}) \in \Theta \subset \mathbb{R}^p$, and for a fixed set of points $s_1, \dots, s_d \in S$, we have $Z = (W(s_1), \dots, W(s_d)) \sim \mathcal{N}(\mathbf{0}, \Sigma_{\theta})$, with $(\Sigma_{\theta})_{ij} = C_{\theta}(\|s_i - s_j\|)$. The following two specific examples of covariance functions will be considered in later sections.

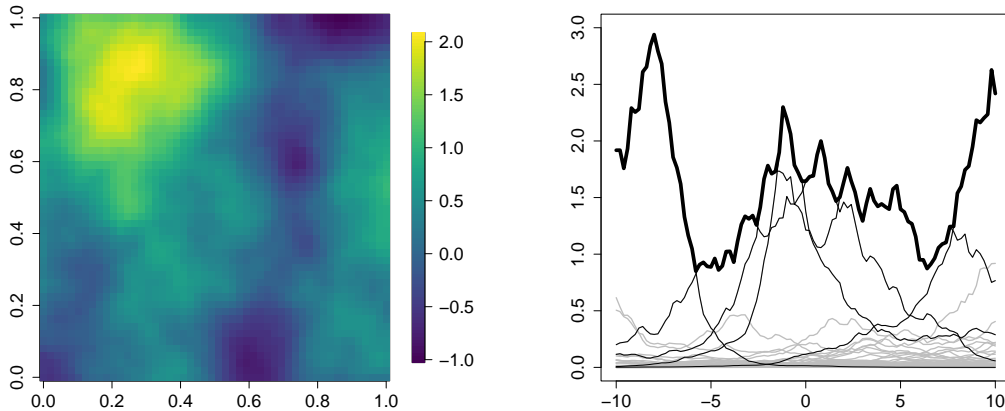


Figure 3: Left: realization of a Matérn random field in $k = 2$ dimensions with $\lambda = 0.2$ and $\nu = 1.5$. Right: representation (11) of a max-stable process in $k = 1$ dimension; the max-stable processes (thick black line) is constructed from extremal functions (gray lines) that contributed to the pointwise maximum (thin back lines).

The powered exponential model is a Gaussian random field with parameters $\tilde{\theta} = (\lambda, \alpha) \in (0, \infty) \times (0, 2)$ and continuous part of the covariance function

$$\tilde{C}_{\tilde{\theta}}(h) = \exp\{-(h/\lambda)^\alpha\}, \quad h \geq 0. \quad (8)$$

The Matérn model is a Gaussian random field with continuous part of the covariance

$$\tilde{C}_{\tilde{\theta}}(h) = \frac{2^{1-\nu}}{\Gamma(\nu)} \left(\sqrt{2\nu} \frac{h}{\lambda}\right)^\nu K_\nu\left(\sqrt{2\nu} \frac{h}{\lambda}\right), \quad h \geq 0, \quad (9)$$

where Γ is the Gamma function and K_ν is the Bessel function of the second kind of order ν . In line with Gerber and Nychka [2021], we consider a fixed smoothness parameter $\nu > 0$, leaving the range parameter $\lambda \in (0, \infty)$ as the only free parameter; see the left-hand side of Figure 3 for a realization of the Matérn field.

For Gaussian random fields evaluated at many spatial locations likelihood estimation can become prohibitively expensive [Rue and Held, 2005]. The simulation of a reasonable amount samples from such processes remains however feasible.

2.3.2 Max-stable distributions

Max-stable distributions arise naturally in the study of extreme values of random processes. For independent copies U_i , $i \in \mathbb{N}$, of some stochastic process $U = \{U(s) : s \in S\}$ on S , a max-stable process W is the only possible limit in distribution of normalized maxima

$$W(s) = \lim_{m \rightarrow \infty} a_m(s)^{-1} \max_{i=1, \dots, m} \{U_i(s) - b_m(s)\}, \quad s \in S, \quad (10)$$

where $a_m(s) > 0$ and $b_m(s) \in \mathbb{R}$ are suitable normalizing functions, and where the convergence is meant in the sense of finite dimensional distributions [de Haan, 1984]. Any max-stable process has the stochastic representation

$$W(s) = \max_{i \in \mathbb{N}} \xi_i Y_i(s), \quad s \in S, \quad (11)$$

where ξ_i are the points of a Poisson point process with intensity $\xi^{-2} d\xi$, and Y_i , $i \in \mathbb{N}$, are independent copies of a random field Y , the so-called extremal functions [Dombry et al., 2012]. The right-hand side of Figure 3 illustrates this representation.

Choosing suitable families of extremal function Y yields parametric models of max-stable processes. The most popular spatial model in the literature is the class of Brown–Resnick processes [Brown and Resnick, 1977, Kabluchko et al., 2009], where

$$Y(s) = \exp\{V(s) - \gamma(s)\}, \quad (12)$$

is an intrinsically stationary Gaussian random field satisfying $V(0) = 0$ almost surely, and with variogram $\gamma_{c,\alpha}(h) = ch^\alpha$. The parameter space for this model is $\theta = (c, \alpha) \in \Theta = (0, \infty) \times (0, 2)$, and the marginal distributions are unit Fréchet. The finite dimensional margin of the Brown–Resnick process W at locations $s_1, \dots, s_d \in S$ is a max-stable random vector $Z = (W(s_1), \dots, W(s_d))$ that follows a so-called Hüsler–Reiss distribution [Hüsler and Reiss, 1989]. Similarly to normal distributions, the density of this model can be expressed in terms of a precision matrix [Hentschel et al., 2024] and is used for graphical modeling of multivariate extremes [Engelke and Hitz, 2020].

For a finite set as the domain $S = \{1, \dots, d\}$ in (10) we obtain a d -dimensional max-stable distribution Z . A classical parametric example is the logistic model [Gumbel, 1960] with unit Fréchet margins and distribution function

$$\mathbb{P}_\theta(Z_1 \leq z_1, \dots, Z_p \leq z_d) = \exp\left(-\left(z_1^{-\frac{1}{\theta}} + \dots + z_d^{-\frac{1}{\theta}}\right)^\theta\right), \quad (13)$$

which is parametrized by a single parameter $\theta \in \Theta = (0, 1)$.

The density of max-stable distributions is computationally intractable, since in d dimensions it is a sum of B_d terms, where B_d is the d th Bell number [Wadsworth, 2015]. This number grows super-exponentially in d and makes full-likelihood inference impossible even in moderate dimensions. The reason is that many different extremal functions in the representation (11) can contribute to the maximum, explaining the explosion of terms; see the right-hand side of Figure 3 for an illustration and Dombry et al. [2016] for details.

While likelihood inference for max-stable processes is difficult, exact simulation is possible and computationally relatively efficient. In fact, the algorithm introduced in Dombry et al. [2016] requires in average the simulation of d extremal functions V to generate one realization of a d -dimensional max-stable random vector. For Brown–Resnick processes, for instance, this has to be multiplied by the simulation cost of a d -dimensional normal distribution.

3 Bayes risk

In this section we establish conditions for the Bayes Risk $R(f_m^*)$ to vanish. This term only depends on the model family \mathcal{P}_θ , the prior distribution Π of θ , and the number m of i.i.d. samples $(z^1, \dots, z^m) = z$ to which the Bayes estimator is applied. The approximation quality of neural networks f_ϕ or the number N of samples used to train each network are irrelevant at this stage, as they do not affect the Bayes estimator $f^*(z)$.

Consequently, we can build on well-known results from Bayesian estimation theory, and in particular the Bernstein–von Mises theorem.

Theorem 3.1 (Bernstein–von Mises; Theorem 10.8 in van der Vaart [1998]). *Let $\{p_\theta\}_{\theta \in \Theta}$ be differentiable in quadratic mean at θ_0 with non-singular Fisher information matrix I_{θ_0} . Suppose that for every $\varepsilon > 0$ there exists a sequence of tests $(t_m^\varepsilon)_{m \in \mathbb{N}}$ with*

$$\mathbb{E}_{\theta_0}[t_m^\varepsilon] \rightarrow 0, \quad \text{and} \quad \sup_{\|\theta - \theta_0\| > \varepsilon} \mathbb{E}_\theta[1 - t_m^\varepsilon] \rightarrow 0, \quad \text{as} \quad m \rightarrow \infty. \quad (14)$$

Let (Z_1, Z_2, \dots) be i.i.d. with respect to p_{θ_0} and parameter $\theta_0 \in \Theta$. Moreover, suppose the loss function ℓ satisfies $\ell(\theta, \theta_0) = \|\theta - \theta_0\|^p$ for some $p \geq 1$ and $\int_\Theta \|\theta\|^p \pi(\theta) d\theta < \infty$. Let the density π of the prior distribution be continuous and positive in a neighborhood of θ_0 . Then, the Bayes estimator is asymptotically normal and efficient.

Theorem 3.1 allows conclusions about the point-wise risk for a given true parameter θ_0 . In order to extend these to the integrated Bayes risk $R(f_m^*)$, we add the following assumption on the parameter space Θ .

Assumption 3.2. *The parameter space Θ of the considered model is compact. In particular, there exists $B < \infty$ with $\|\theta\|_\infty < B$ for all $\theta \in \Theta$.*

This assumption will be used in many of the later results. Some of these only require boundedness, such as the following corollary about the Bayes risk $R(f_m^*)$, but for simplicity we will always assume compactness throughout the paper. Even though many models originally have unbounded or non-compact parameter spaces, we can restrict them to compact subsets thereby satisfying Assumption 3.2. In practice, this is a very natural restriction, as the range of “reasonable” parameter values is often known in advance.

Corollary 3.3. *(See Proof.) Let Θ be bounded (implied by Assumption 3.2), consider the quadratic loss from (4), and let the conditions from Theorem 3.1 be satisfied for some $\theta_0 \in \Theta$. Then*

$$\lim_{m \rightarrow \infty} R_{\theta_0}(f_m^*) = 0. \quad (15)$$

If they are satisfied for all $\theta \in \Theta$, then the integrated risk converges as well:

$$\lim_{m \rightarrow \infty} R(f_m^*) = 0. \quad (16)$$

The condition on the prior distribution in Theorem 3.1 can be satisfied by a suitable choice for π such as the continuous uniform distribution, for instance; in the sequel we will assume that the prior distribution is chosen in such a way. The remaining conditions from Theorem 3.1 and Corollary 3.3 have to be checked on a per-model basis. The results below confirm the conditions for the examples given in Section 2.3.

Lemma 3.4. *(See Proof.) The Gaussian random field models with powered exponential covariance function (8) and the Matérn covariance function (9), evaluated at a fixed set of points s_1, \dots, s_d , satisfy the conditions of Corollary 3.3 if the points are located such that there are at least two distinct, non-zero distances between them.*

For max-stable distributions, the following result is obtained by using the tests constructed in Dombry et al. [2017b].

Lemma 3.5. *(See Proof.) The logistic model from (13) and the Brown–Resnick model from (12) satisfy the conditions of Corollary 3.3 if the points are located such that there are at least two distinct, non-zero distances between them.*

4 Approximation error

In the previous section we showed that, under suitable assumptions, the risk $R(f_m^*)$ of the Bayes estimator vanishes. In the context of neural estimators, this estimator is approximated by a neural network, giving rise to the approximation error. Assuming the quadratic loss function from (4), this error can be expressed as

$$R(\phi_m^*) - R(f_m^*) = \mathbb{E}[\|f_{\phi_m^*}(Z) - f_m^*(Z)\|_2^2]; \quad (17)$$

see Appendix A.2 for details. Note that without any restrictions, the concept of an “optimal” network ϕ_m^* is not well-defined. Instead, we show that the error term above can be made arbitrarily small by using a suitable activation function, large enough architecture for a given input size $z = (z^1, \dots, z^m)$, and optimal parameter values. The effect of training a model with this architecture using the empirical risk R_N instead of the population risk R is investigated in Section 5.

In order to bound the risk of the considered networks, we make use of the universal approximation theorem. For the sake of specificity, we only consider the ReLU activation function, denoted by σ . However, the results given here and in Section 5 also apply to other commonly used activation functions, possibly with slight modifications.

Theorem 4.1 (Cybenko, 1989). *For every continuous function $f : \mathbb{R}^D \rightarrow \mathbb{R}^p$, $M > 0$, and $\varepsilon > 0$ there exists a shallow neural network parametrization $\phi = (w, \beta)$ with one hidden layer of width $N_1 \in \mathbb{N}$, such that*

$$\sup_{x \in [-M, M]^D} \|f(x) - f_\phi(x)\|_2 < \varepsilon.$$

Example 2.1 provides details for the parametrization of such a shallow network. In order to apply this result—and others like it—to the setting of neural estimators, we need to introduce some assumptions on the considered models.

Assumption 4.2. *For any $m \in \mathbb{N}$, the Bayes estimator function $f_m^*(z) = \mathbb{E}(\theta|Z = z)$ is continuous on \mathcal{Z}^m .*

This assumption ensures that the Bayes estimator function is actually in the class of functions that can be approximated well by neural networks. While the Bayes estimator is usually not available in closed form, the following lemma gives a sufficient condition for its continuity.

Lemma 4.3. *(See Proof.) Consider a compact parameter space Θ and the quadratic loss function from (4). If $p_\theta(z)$ is continuous in θ and z , then $f(z) = \mathbb{E}(\theta|Z = z)$ is continuous.*

The statement of universal approximation in Theorem 4.1 holds only on bounded sets $[-M, M]^D$. We therefore require an assumption that ensures that the observations of Z are, with high probability, eventually contained in a compactum, independently of the parameter θ_0 .

Assumption 4.4. *The model is uniformly tight, that is, for every $\varepsilon > 0$ there exists $M > 0$ such that*

$$\sup_{\theta_0 \in \Theta} \mathbb{P}_{\theta_0} (\|Z\|_\infty > M) < \varepsilon.$$

While the stronger assumption of bounded realizations of the model would imply the above condition, it would be too restrictive for the examples of Gaussian processes or extreme value models described in Section 2.3. Instead, the error incurred by observations from outside the compactum $[-M, M]^D$ can be controlled by Assumption 3.2, which ensures that the model parameters, and hence the corresponding loss function, are bounded.

The following example illustrates that Assumption 4.4 is in some cases implied by Assumption 3.2, similar statements hold for the examples in Section 2.3.

Example 4.5. *The model $\mathcal{P}_\theta = \mathcal{N}(\mu, \sigma^2)$, with parameter $\theta = (\mu, \sigma) \in \Theta \subset \mathbb{R} \times (0, \infty)$ is tight if and only if Θ is bounded.*

Combining these assumptions and the universal approximation theorem, we get the following result.

Proposition 4.6. *(See Proof.) Suppose Assumptions 3.2, 4.2, and 4.4 hold. Then, for every $\varepsilon > 0$, there exists a ReLU neural network with two hidden layers and parameters ϕ_m^* that has bounded outputs and satisfies*

$$R_{\theta_0}(\phi_m^*) - R_{\theta_0}(f_m^*) = \mathbb{E}_{\theta_0} [\|f_{\phi_m^*}(Z) - f_m^*(Z)\|_2^2] < \varepsilon, \quad (18)$$

for all $\theta_0 \in \Theta$; here the expectation is over $Z \sim \mathcal{P}_{\theta_0}$ for a fixed value of θ_0 . Furthermore, the same network satisfies

$$R(\phi_m^*) - R(f_m^*) = \mathbb{E} [\|f_{\phi_m^*}(Z) - f_m^*(Z)\|_2^2] < \varepsilon, \quad (19)$$

where the expectation is over $\theta \sim \pi$ and $Z \sim \mathcal{P}_\theta$.

Since Theorem 4.1 guarantees the existence of a uniformly good approximation, the network parameters ϕ_m^* do not depend on θ_0 . Hence, we obtain the result in (19) for the integrated risk R by integrating out the prior distribution $\theta \sim \pi$ in (18). The network architecture used in the proof of Proposition 4.6 has two hidden layers: one for the actual approximation of the Bayes estimator f^* , and one to make sure the output is contained in the bounded set $[-B, B]^p$. By Assumption 3.2, this interval contains the entire parameters space Θ , and the clipping does therefore not impact the approximation quality of the network.

As an intermediate theoretical result, we can find a sequence of neural network parametrization ϕ_m^* for m replicates such that

$$R_{\theta_0}(\phi_m^*) \rightarrow 0 \quad R(\phi_m^*) \rightarrow 0, \quad m \rightarrow \infty,$$

that is, the pointwise and the joint risks of the optimal neural networks converge to zero. This follows by choosing different ε_m in (18) and (19) for each value of m such that $\varepsilon_m \rightarrow 0$ for $m \rightarrow \infty$, and using Corollary 3.3 for convergence of the Bayes risk. In practice, this result is not applicable directly since the optimal network is unknown. In the next section we therefore study the generalization error that quantifies how far the estimated parameters ϕ_m^N are from the optimal ϕ_m^* .

Remark 4.7. *Theorem 4.1 on universal approximation states the existence of a shallow neural network for arbitrary good approximation only. Poggio et al. [2017] show that in the absence of additional assumptions on the smoothness of the function, the complexity of a shallow neural network is at least exponential in the input size when the activation function is not a polynomial. In the literature, this is referred to as the curse of dimensionality. To overcome this, it is believed that deep neural networks are necessary. Poggio et al. [2017] also argue that deep neural networks can more efficiently approximate functions with hierarchical compositional structure, leading to significantly reduced complexity compared to shallow networks; see also Schmidt-Hieber [2020]. Yarotsky [2017] constructs approximation schemes for deep ReLU networks, where the required network complexity depends explicitly on the smoothness of the target function. As the function’s smoothness increases, the exponential dependence on the input dimension can be mitigated. However, when the smoothness is insufficient, the number of neurons per layer can still grow exponentially with dimension.*

We conclude this section by verifying the conditions for Proposition 4.6 to hold for the models considered in Section 2.3. We have to check Assumptions 3.2, 4.2, and 4.4. The applicability of Assumption 3.2 is discussed following its statement, and the other two assumptions have to be checked on a per-model basis, which is done below.

Lemma 4.8. *(See Proof.) When restricted to a compact parameter space Θ (Assumption 3.2), the powered exponential model from (8) and the Matérn model from (9) satisfy Assumptions 4.2 and 4.4.*

Lemma 4.9. *(See Proof.) When restricted to a compact parameter space Θ , the logistic model from (13) and the Brown–Resnick model from (12) satisfy Assumptions 4.2 and 4.4.*

More generally, any family of multivariate distributions with standardized univariate margins is uniformly tight, as the parameter only affects the multivariate interactions, but not the overall magnitude of the observations. For Gaussian random fields, it is sufficient to assume that the covariance function is bounded over Θ , to guarantee tightness of the model.

5 Generalization error

In this section we consider the generalization error and its decomposition in (6) and (7). As discussed in Section 2.2, this error term is mainly driven by the term $R(\phi_m^N) - R_N(\phi_m^N)$, which captures the difference between the true risk R and the empirical risk R_N , with respect

to which the neural network ϕ_m^N is trained. The remaining terms in (7) are bounded with conventional techniques in the proof of Corollary 5.5.

In order to bound this error term, we use the concept of robust algorithms, introduced by [Xu and Mannor \[2012\]](#). Throughout, they assume that the loss function is upper bounded by some $E < \infty$. We also consider this assumption to be satisfied, since Assumption 3.2 implies $\|\theta\|_\infty < B$, and the output $\hat{\theta}$ of a neural network can be restricted to be bounded by B , as described in the proof of Proposition 4.6, yielding a maximal quadratic loss of

$$\|\theta - \hat{\theta}\|_2^2 \leq 4pB^2 := E.$$

Applying results based on robustness directly to neural networks requires the input and output space of the network to be compact. In our setting, this is satisfied for the output space, since Assumption 3.2 implies that Θ is bounded, but is not a sound assumption for the input space, which consists of samples from the support of the analyzed distribution. We therefore employ the concept of pseudo-robustness, also introduced by [Xu and Mannor \[2012\]](#), which can be used together with the Assumption 4.4 of a uniformly tight model to bound the error incurred by input values coming from outside a certain compact set.

Considering two sets \mathcal{X} and \mathcal{Y} , an algorithm A is a mapping from a training sample $s = (x, y) \in (\mathcal{X} \times \mathcal{Y})^N$ to a function $A_s \in \mathcal{F}$, where \mathcal{F} is a subset of functions $f : \mathcal{X} \rightarrow \mathcal{Y}$.

Example 5.1. *In the general setting of neural estimators we have that $\mathcal{X} = \mathcal{Z}^m$ is the space of m -dimensional samples and $\mathcal{Y} = \Theta \subset \mathbb{R}^p$ is the Euclidean space containing the parameter space. The set of functions \mathcal{F} is the set of neural networks considered in the training; one example of such as function class is the set of single-layer, fully-connected, feedforward neural networks in Example 2.1. For a set of training points $s = ((z_1, \theta_1), \dots, (z_N, \theta_N)) \in (\mathcal{X} \times \mathcal{Y})^N$, the algorithm A then is the empirical risk minimizer $s \mapsto \phi_m^N$ as defined in (2).*

The following definition is a simplified version of Definition 5 in [Xu and Mannor \[2012\]](#).

Definition 5.2 (Pseudo-Robustness). *Let $K \in \mathbb{N}$, $\varepsilon \geq 0$, and $\hat{N} : (\mathcal{X} \times \mathcal{Y})^N \rightarrow \{1, \dots, N\}$. An algorithm $A : s \mapsto A_s$ is called $(K, \varepsilon, \hat{N})$ -pseudo-robust if $\mathcal{X} \times \mathcal{Y}$ can be partitioned into K disjoint sets $\{C_i\}_{i=1, \dots, K}$, such that for all $s \in (\mathcal{X} \times \mathcal{Y})^N$, there exists a subset of training samples, indexed by $\hat{I} \subseteq \{1, \dots, N\}$ with $|\hat{I}| = \hat{N}(s)$, that satisfies the following: For all $i \in \{1, \dots, K\}$, $j \in \hat{I}$, satisfying $s_j = (x_j, y_j) \in C_i$, and any $(x', y') \in C_i$, it holds that*

$$|\ell(A_s(x_j), y_j) - \ell(A_s(x'), y')| \leq \varepsilon.$$

Generally speaking, the value of \hat{N} needs to be close to N in order to obtain relevant error bounds from the results below. If $\hat{N} \equiv N$, the algorithm is called (K, ε) -robust; see Definition 2 in the same paper. Note that (pseudo-)robustness itself is a deterministic property. However, if the input to the algorithm is a random variable S consisting of N i.i.d. samples from the joint distribution of random variables X and Y , each taking values in $\mathcal{X} \times \mathcal{Y}$, Theorem 4 in [Xu and Mannor \[2012\]](#) shows that the generalization error of a $(K, \varepsilon, \hat{N})$ -pseudo-robust algorithm can be bounded with probability $1 - \delta$ for any $\delta \in (0, 1)$ by

$$|R(A_S) - R_N(A_S)| \leq \frac{\hat{N}(S)}{N} \varepsilon + E \left(\frac{N - \hat{N}(S)}{N} + \sqrt{\frac{2K \log(2) + 2 \log(\frac{1}{\delta})}{N}} \right). \quad (20)$$

The error bound in this result still depends on the realization of S through the number $\hat{N}(S)$. In the general case, \hat{N} can be an arbitrary function, however, in our setting it will be determined by the number of samples (X, Y) that fall into a certain set $\mathcal{X}' \times \mathcal{Y}'$. Approximating the ratio of “outliers”, $(N - \hat{N}(S))/N$, by its expectation and bounding the resulting error term then yields the following result.

Lemma 5.3. (See Proof.) Let $A : s \mapsto A_s$ be a $(K, \varepsilon, \hat{N})$ -pseudo-robust algorithm, where $\hat{I}(s) = \{i \mid (x_i, y_i) \in \mathcal{X}' \times \mathcal{Y}'\}$ for some sets $\mathcal{X}' \subseteq \mathcal{X}$ and $\mathcal{Y}' \subseteq \mathcal{Y}$, and $\hat{N}(S) = |\hat{I}(s)|$. Then, for any $\delta \in (0, 1)$ the generalization error can be bounded with probability at least $1 - \delta$ by

$$|R(A_S) - R_N(A_S)| \leq \varepsilon + E \left(\mathbb{P}((X, Y) \notin \mathcal{X}' \times \mathcal{Y}') + \sqrt{\frac{\log(\frac{2}{\delta})}{2N}} + \sqrt{\frac{2K \log(2) + 2 \log(\frac{2}{\delta})}{N}} \right).$$

Lastly, to apply the concept of robustness to neural estimators, we need to establish that algorithms yielding neural networks are pseudo-robust. To this end, the following result is a modification of Example 7 in Xu and Mannor [2012], considering the quadratic loss function and the ReLU activation function. We consider the set of restricted (fully connected feedforward) neural networks f_ϕ with L layers, that map from $\mathcal{X} \subseteq \mathbb{R}^{m_d}$ to a set $\mathcal{Y} \subseteq \mathbb{R}^p$, bounded by $B < \infty$. These networks can be parametrized by

$$\Phi^{\alpha, L} = \left\{ \phi = (w, \beta) \mid N_l \leq \alpha, \sum_{i=1}^{N_l} |w_{i,j}^l| \leq \alpha, \forall l = 1, \dots, L \wedge |f_\phi(x)| \leq B, \forall x \in \mathcal{X} \right\}, \quad (21)$$

for some $\alpha \geq 1$, where N_l the size of the l th layer for $l = 1, \dots, L$, and $w^{(l)} \in \mathbb{R}^{N_l \times N_{l+1}}$ the corresponding weight matrix. The first inequality is imposed to ensure existence of the minimizer in (23) below.

Lemma 5.4. (See Proof.) Let \mathcal{Y} be bounded by $B < \infty$, let \mathcal{X}' be a bounded subset of \mathcal{X} , and fix $\alpha > 0$. Then, an algorithm taking values in $\mathcal{F} = \{f_\phi : \mathcal{X} \rightarrow \mathcal{Y} \mid \phi \in \Phi^{\alpha, L}\}$ is $(K(\gamma), c\gamma, \hat{N})$ -pseudo-robust for all $\gamma > 0$, where with

$$\begin{aligned} K(\gamma) &= \mathcal{N}(\gamma/2, \mathcal{X}' \times \mathcal{Y}, \|\cdot\|_\infty) \\ c &= 4B\rho(\alpha^L + 1) \\ \hat{N}(S) &= \#\{i \mid (x_i, y_i) \in \mathcal{X}'\}, \end{aligned}$$

where $\mathcal{N}(r, \mathcal{S}, \|\cdot\|)$ denotes the covering number of a set \mathcal{S} with respect to the norm $\|\cdot\|$, using balls of radius r .

The above results allows us to bound the generalization error of neural estimators under some restrictions. In our setting, \mathcal{Y} is already bounded by the assumption of a bounded parameter space Θ (Assumption 3.2) and by choosing $\mathcal{X}' = [-M, M]^{m_d}$ the probability

$$\mathbb{P}(X \notin \mathcal{X}') = \mathbb{P}(\|Z\|_\infty > M) \quad (22)$$

can be controlled using model tightness from Assumption 4.4.

In order to satisfy the restriction from (21), the absolute sum of the weights in each layer needs to be bounded by α , which is not guaranteed by the empirical risk minimizer ϕ_m^N . However, we can consider the restricted optimizer $\phi_m^{N, \alpha}$ defined as

$$\phi_m^{N, \alpha} = \arg \min_{\phi \in \Phi^{\alpha, L}} R_N(\phi), \quad (23)$$

and choose $\alpha = \alpha(N)$ to increase in N at a certain rate. Here, the architecture, and in particular the number of input samples m and layers L , are fixed according to the architecture of the ‘‘optimal’’ neural network ϕ_m^* from Proposition 4.6. For large enough N , the weights ϕ_m^* are admissible for the restricted empirical risk minimizer, and robustness results can be used to show that $R(\phi_m^{N, \alpha(N)})$ is close to $R(\phi_m^*)$.

Putting the above considerations together yields the following result.

Corollary 5.5. (See Proof.) Suppose Assumptions 3.2 and 4.4 hold. Consider a fixed network architecture with L layers, let ϕ_m^* be its optimal weights with respect to risk R ,

and let $\phi_m^{N,\alpha(N)}$ be the restricted empirical risk minimizer defined in (23). Assume that the output of the network ϕ_m^* is bounded by the same B as in (21) and Assumption 3.2. Then there exists $N_1 \in \mathbb{N}$ and a functional ζ such that for every $\delta \in (0, 1)$ we have $\zeta(\delta, N) \rightarrow 0$ as $N \rightarrow \infty$, and for any $N \geq N_1$ it holds with probability at least $1 - \delta$

$$R(\phi_m^{N,\alpha(N)}) - R(\phi_m^*) < \zeta(\delta, N).$$

The rate of $\alpha(N)$ and the functional ζ are given explicitly in the proof.

Note that the approach from Corollary 5.5 cannot be used to bound $R(\phi_m^N)$, the risk of the unrestricted empirical risk minimizer, since its weights change with N , and, in particular, might diverge at a faster rate than required to obtain the bound in the corollary. Restriction of the empirical minimizer by penalizing the size of the weights as in (21) is a well-known regularization technique in machine learning which has been shown to work well in practice [Goodfellow et al., 2016]. It is therefore natural to consider the risk of the estimator $\phi_m^{N,\alpha(N)}$ rather than the empirical risk minimizer ϕ_m^N .

Remark 5.6. Lemmas 4.8 and 4.9 show that Assumption 4.4 is satisfied for the examples from Section 2.3, no further assumptions on the distribution of the data need to be checked.

6 Statistical guarantees for neural estimators

6.1 Consistency results

The previous sections we have analyzed the different components of the risk of a neural estimator. This involved both statistical aspects of the considered model class and properties of the neural networks used to construct the estimator. We can now combine these results to obtain asymptotic guarantees for neural estimators. In particular, putting together Corollary 3.3, Proposition 4.6, and Corollary 5.5, and choosing the training sample size $N(m)$, the size of the neural network $\alpha(m)$ and the probability $\delta(m)$ appropriately, we get that the risk of the neural estimator converges to zero as $m \rightarrow \infty$. As above, we consider the quadratic loss function and use the ReLU activation function in the neural network.

Theorem 6.1. (See Proof.) Suppose that the conditions from Theorem 3.1 as well as Assumptions 3.2, 4.2, and 4.4 hold. For input sample size m , consider the network architecture implied by ϕ_m^* from Proposition 4.6 for $\varepsilon_m = R(f_m^*)$. For replicate count m , training set size N , and $\alpha > 0$, let $\phi_m^{N,\alpha}$ denote the restricted empirical risk minimizer from (23). Then, there exist $\alpha(m)$ and $N(m) \rightarrow \infty$ such that

$$R(\phi_m^{N(m),\alpha(m)}) \xrightarrow{p} 0, \quad m \rightarrow \infty. \quad (24)$$

The probability in the above results is over the distribution of the training data. Using the boundedness of the parameter space Θ , and hence of the loss function, we also obtain the following convergences.

Corollary 6.2. (See Proof.) Consider the assumptions and notation of Theorem 6.1. Write ϕ_m short for $\phi_m^{N(m),\alpha(m)}$, and let S_m denote the training sample used to train ϕ_m . Then we have the following convergences

$$f_{\phi_m}(Z) \xrightarrow{L^2} \theta, \quad f_{\phi_m}(Z) \xrightarrow{p} \theta, \quad (25)$$

where the left-hand sides are random variables with respect to the joint distribution of S_m, θ, Z , and the θ on the right-hand sides is a random variable itself.

With respect to the pointwise risk R_θ , we have

$$R_\theta(\phi_m) \xrightarrow{L^1} 0, \quad R_\theta(\phi_m) \xrightarrow{p} 0.$$

The two expressions are random variables with respect to the distribution of S_m, θ .

The convergences in (25) can be seen as consistency of the neural estimator in a Bayesian sense. In general, when conditioning on a single fixed $\theta_0 \in \Theta$, the true parameter in the frequentist setting, the convergence results need not hold. It is an open question whether one can find suitable additional conditions under which such classical pointwise consistency guarantees hold.

Considering the relevant assumptions, checked in Lemmas 3.4, 3.5, 4.8, and 4.9, we conclude that the risk of neural Bayes estimators applied to the examples of Gaussian random fields and max-stable distributions from Section 2.3 converges to zero in the sense of Theorem 6.1 and Corollary 6.2.

6.2 Discussion of convergence rates and Bayes efficiency

Theorem 6.1 and Corollary 6.2 state that neural estimators are consistent in a Bayesian sense. In order to show that neural estimators can be fully efficient compared to the Bayes estimator, we need that the risk ratio satisfies

$$\frac{R(\phi_m^{N(m), \alpha(m)})}{R(f_m^*)} = 1 + \frac{R(\phi_m^*) - R(f_m^*)}{R(f_m^*)} + \frac{R(\phi_m^N) - R(\phi_m^*)}{R(f_m^*)} \xrightarrow{p} 1, \quad m \rightarrow \infty. \quad (26)$$

We discuss the rates of the different terms and conditions that balance the network complexity, the training sample size and properties of the statistical model to ensure this convergence.

Let $\varepsilon_m = R(f_m^*)$ denote the Bayes risk for estimation based on m replicates. For a given m , the approximation error $R(\phi_m^*) - R(f_m^*)$ can be made arbitrarily small because of bound (19) in Proposition 4.6. We choose as target for this error any sequence η_m such that $\eta_m/\varepsilon_m \rightarrow 0$. The size of the neural network ϕ_m^* that achieves this approximation grows both in the input dimension m and the required approximation accuracy η_m . For the shallow neural networks considered here, and under mild assumptions on the target function f_m^* , this growth can be linear in η_m^{-m} [Yarotsky, 2017]. Other architectures could improve the required network size substantially, both in practice [e.g., Sainsbury-Dale et al., 2023] and in theory.

Once the network architecture is fixed for every $m \in \mathbb{N}$, we control the generalization error $R(\phi_m^N) - R(\phi_m^*)$ by suitable choices of the training sample size $N(m)$ and the size of the neural network $\alpha(m)$ in the parameterization (21). We first observe that the tail heaviness of the statistical model is a driving factor in the generalization error, where heavier tails with larger probabilities $\mathbb{P}(\|Z\|_\infty > M)$ in (22) for large M lead to larger errors. To compensate, we need to choose suitably large training sizes $N(m)$. For instance, for sub-Gaussian tails, including the Gaussian model in Section 2.3.1, this implies that $N(m)$ grows faster than $\log(\eta_m^{-1})^{2(md+p)}$. For heavier tails, such as the polynomial tail decay of the max-stable models in Section 2.3.2, the training size should grow faster with rate $(\eta_m)^{-C(md+p)}$ for some constant C .

The network size $\alpha(m)$ needs to increase fast enough such that the optimal neural network ϕ_m^* is contained in the admissible set (21). Larger and more expressive networks are more prone to overfitting and therefore require larger training sizes $N(m)$ to control the generalization error. A suitable choice of $\alpha(m)$ and a sequence $N(m)$ that asymptotically grows faster than $\eta_m^{-Km^2}$ as $m \rightarrow \infty$, for a large enough constant K , ensures such a trade-off. The convergence in (26) then holds if the tail of the model Z is not too heavy, such as a sub-Gaussian or polynomial tail.

A detailed rate discussion can be found in Appendix A.5.

7 Simulation study

We conduct several numerical experiments in order to illustrate the behavior of the neural estimator. This will help to better understand the implication of the theoretical guarantees

on the different risk terms in a practical application. We concentrate here on the max-stable logistic model introduced in (13), fixing the dimension to $d = 5$. The prior distribution Π for the model parameter θ is always uniform over $(0, 1)$, and we consider different numbers of simultaneous replicates $m \in \{1, \dots, 10\}$. In this relatively low dimension, it is still possible to obtain the Bayes estimator exactly through the Markov chain Monte Carlo (MCMC) algorithm proposed in Dombry et al. [2017b], which we will use as the baseline throughout.

Additional simulations for the illustrative example of linear model fitting can be found in Appendix C.

7.1 Comparison of estimators

In this section we illustrate the potential of the neural estimator $\hat{\theta}_N = f_{\phi_m^N}(Z)$ to effectively approximate the Bayes estimator $\hat{\theta}_B = f_m^*(Z)$ obtained by MCMC. We choose a large number $N = 10^4$ of training samples to mostly ignore the generalization error in (6). Moreover, using the automated machine learning approach [LeDell and Poirier, 2020], we perform an extensive grid search over a set Φ of many different architectures to minimize the approximation error.

We train the models through regularization techniques such as dropout. Although our theoretical analysis and sample guarantees only hold for the empirical risk minimizer, there are several reasons to use regularization techniques in practice. First, due to a complex landscape of local minima, standard algorithms take very long to converge to the true global minimum and might be stuck in local minima and flat regions. Therefore, it can be computationally very hard to find the empirical risk minimizer. Second, the estimator resulting from regularization-based training usually performs better on the test data set than the true minimizer ϕ_m^N .

To evaluate the performance of the neural estimator, we generate 500 independent test samples of θ from the prior distribution Π . Theoretical results suggest a decreasing risk for the MCMC Bayes estimator as m increases, and similar behavior is expected for the neural estimator, provided it has sufficient approximation capacity. The results in Figure 4 show that the optimal neural estimator approximates the Bayes estimator well. Both estimators have a strongly decreasing risk as m increases.

7.2 Evaluation of training data effects

We study more carefully the effect of different amounts of training samples N and simultaneous replicates m on the terms of the risk decomposition (6). In Figure 5 we track all risks that appear in this decomposition, implicitly also containing the approximation error and the generalization error as the differences of relevant curves. All population risks are approximated by the risk on a large test data set.

In addition to the risk of the non-regularized, empirical risk minimizer ϕ_m^N , we also include the regularized estimator $\tilde{\phi}_m^N$, since it is typically applied in practice and improves the risk especially for small N . The optimal neural estimator ϕ_m^* is again computed with a large N and by a grid search over many architectures.

We observe that the optimal neural estimator has a comparable risk to the Bayes risk across different numbers of replicates $m = 1, \dots, 10$, confirming the results of the simulations in the previous section. Note that the Bayes risk satisfies by definition that $R(f_m^*) \leq R(\phi_m^*)$, and violations of this in the figure may be due to numerical instability of the MCMC approximation.

The non-regularized and the regularized neural estimator constructed on a small training set of size $N = 100$ seem to overfit and exhibit a large generalization error, especially for a growing number of replicates m . Following our theoretical results, the reason is that N is not large enough compared to m . This is usually not a problem since simulation of the model should be relatively cheap, and we can use larger numbers of training samples. Indeed, for $N = 1000$ both neural estimators perform better. The risk of the regularized estimator has

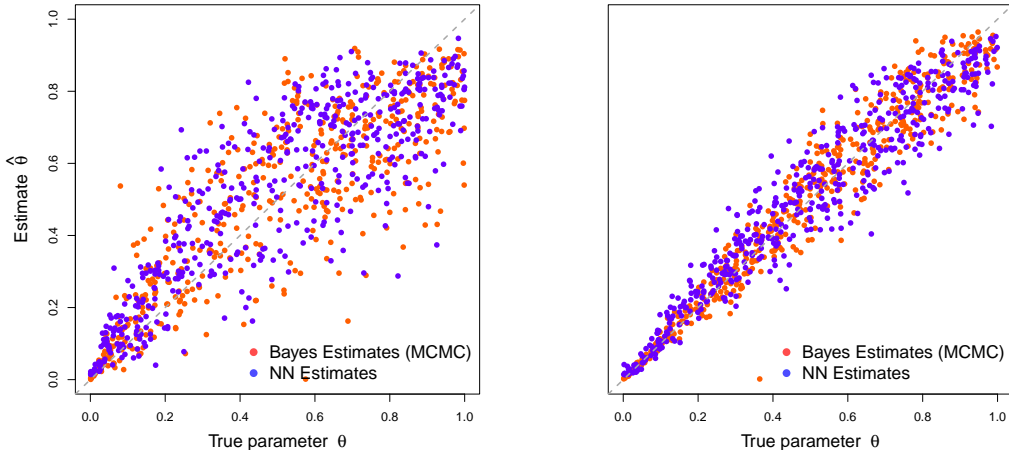


Figure 4: Performance of MCMC Bayes estimator and optimal neural estimator for $m = 1$ (left) and $m = 10$ (right) simultaneous samples, evaluated on 500 test data points with parameters θ sampled from the uniform prior Π on $(0, 1)$. The neural estimator was trained with a large number of simulated training samples N and optimized over different network architectures.

a smaller generalization error and quickly approaches the Bayes risk. This confirms that our theoretical results on the empirical risk minimizer are conservative compared to the regularized estimators usually applied in practice, which typically have even lower risks and potentially better convergence rates.

7.3 Generalization error decomposition

Following the theoretical results in Section 5, we analyze the decomposition (7) of the generalization error when varying the number of replicates m and the amount of training data N . Figure 6 compares the training risks R_N and the population (or test) risks R of the regularized and non-regularized neural estimators.

Consistent with predictions from Hoeffding’s inequality, the training and test risks of the optimal neural estimator ϕ_m^* are almost identical since no overfitting can occur. Similarly to Figure 5 we see that for $N = 100$ both the regularized and non-regularized neural estimators overfit, that is, the training and test risks have a large gap. This gap diminishes for larger $N = 1000$, but is still present in particular for the non-regularized empirical risk minimizer.

Our theoretical results in Section 6 highlight the importance of scaling the number of training samples N properly with the number of replicates m . Figure 7 studies this interplay for an increasing number of N and $m \in \{1, 10\}$ in case of the regularized estimator. We observe that while the training and test risks are very different for small N , for larger N this difference decreases. Eventually, both the training and test risk converge to the risk of the optimal neural network, and therefore also the Bayes risk. This highlights that a sufficiently large number of training samples N is crucial to ensure good performance of neural estimators. Since neural estimators are applied in scenarios where simulation is much cheaper than estimation, this should not be the main bottleneck. Training neural networks with larger sample size is certainly more expensive, but efficient implementations of backpropagation alleviate this issue. Moreover, this training has to be done only once. Neural estimators are then amortized in the sense that they can be applied to any new data set with m replicates from a distribution \mathcal{P}_θ for any $\theta \in \Theta$. This estimation step is extremely

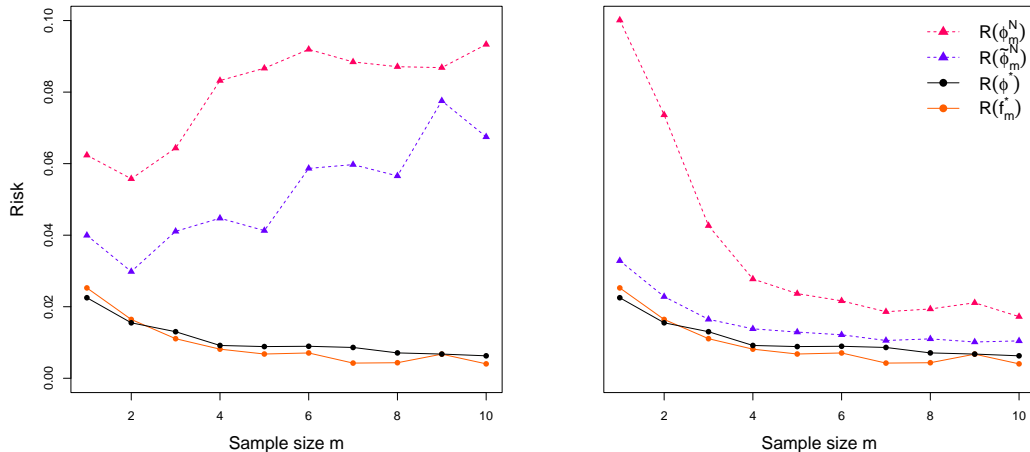


Figure 5: Comparison of risks appearing in decomposition (6) for the Bayes estimator and neural estimators for different number of replicates m . Neural networks were trained on $N = 100$ (left) and $N = 1000$ (right) training samples.

fast since it involves only a forward pass in the trained neural network.

8 Conclusion

The results of this paper are a first step in establishing theoretical guarantees for statistical estimators based on neural networks. Certain bounds that we obtain are conservative since we tried to avoid additional assumptions; see the discussion in Section 6.2. In the theory of statistical learning for deep neural networks, it is known that one can obtain better convergence rates and sharper bounds on the required network complexity under assumptions on the smoothness [Yarotsky, 2017] or a compositional structure of the regression function [Poggio et al., 2017, Schmidt-Hieber, 2020], or if the data generating distribution approximately concentrates on a low-dimensional manifold [Jiao et al., 2023].

The assumption of a compact parameter space Θ is crucial in several of our proofs. This emphasizes the fact that neural networks excel at interpolating data but struggle with extrapolation. In the setting of neural estimators, this means that the whole range of parameters of interest has to be covered with training samples θ_i . This poses an obvious problem in applications where natural bounds on this range are not available. While extrapolation is known to be a difficult problem, there are first statistical approaches to address this issue [Shen and Meinshausen, 2024, Buriticá and Engelke, 2024].

There remain many open questions related to whether our results can be extended to neural estimators that are based on other architectures such as convolutional neural network [Gerber and Nychka, 2021, Lenzi et al., 2021], or that use different loss functions such the quantile loss. Moreover, at the moment it is unclear if neural estimators satisfy some form of asymptotic normality, and whether the popular bootstrap method for uncertainty quantification is consistent.

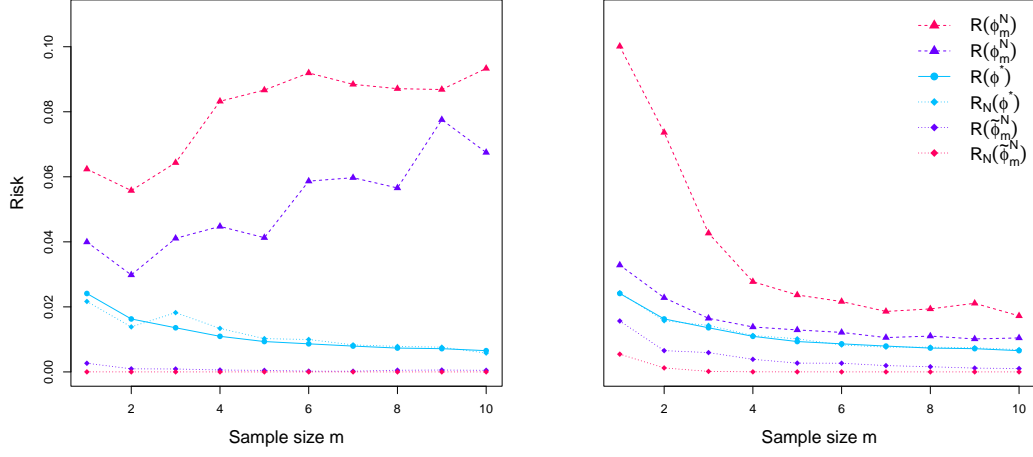


Figure 6: Comparison of risks appearing in decomposition (7) of the generalization error for neural estimators for different number of replicates m . Neural networks were trained on $N = 100$ (left) and $N = 1000$ (right) training samples.

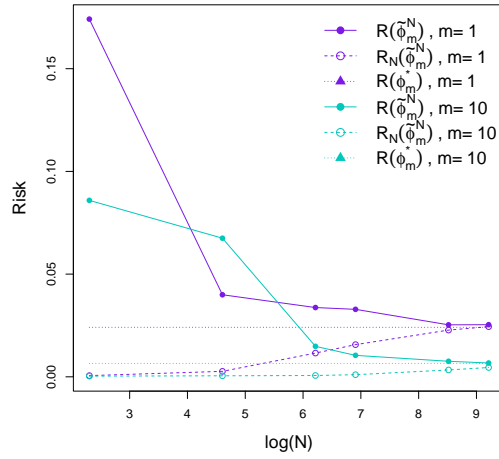


Figure 7: Training and test risks of neural estimators for different number of replicates m and training samples N compared to the optimal neural network risk.

A Proofs of general results

A.1 Bayes Risk

Lemma A.1. (See Proof.) Under the assumptions of Theorem 3.1 for $\theta_0 \in \Theta$, we have

$$\mathbb{P}_{\theta_0}(m^{1/4}\|f_m^*(Z) - \theta_0\|_2 > \varepsilon) \rightarrow 0$$

for all $\varepsilon > 0$.

Proof of Lemma A.1. For simplicity, consider the one-dimensional case. The p -dimensional case then follows by the bound $\|x\|_2 \leq \sqrt{p}\|x\|_\infty$.

Under the assumptions of Theorem 3.1, [van der Vaart, 1998, Theorem 10.8] implies that $\sqrt{m}(f_m^*(Z) - \theta_0)$ converges in distribution to a centered normal distribution with distribution function, say, F . Fix any $\delta > 0$ and let $x = F^{-1}(1 - \delta/4)$. Then, for large m , we have

$$\begin{aligned} \mathbb{P}_{\theta_0}(m^{1/4}(f_m^*(Z) - \theta_0) > \varepsilon) &= \mathbb{P}_{\theta_0}(\sqrt{m}(f_m^*(Z) - \theta_0) > m^{1/4}\varepsilon) \\ &\leq \mathbb{P}_{\theta_0}(\sqrt{m}(f_m^*(Z) - \theta_0) > x) \\ &\leq 1 - \mathbb{P}_{\theta_0}(\sqrt{m}(f_m^*(Z) - \theta_0) < x) \\ &\leq 1 - F(x) + \delta/4 \\ &= \delta/2. \end{aligned}$$

The last inequality follows for large enough m from the convergence in distribution of $\sqrt{m}(f_m^*(Z) - \theta_0)$ to F . By symmetry of the normal distribution, we also have

$$\mathbb{P}_{\theta_0}(m^{1/4}|f_m^*(Z) - \theta_0| > \varepsilon) \leq \delta,$$

and hence the claimed convergence in probability. \square

Proof of Corollary 3.3. First, consider the pointwise result in (15). Under the assumptions of Theorem 3.1 for $\theta_0 \in \Theta$, we have by Lemma A.1 that

$$\mathbb{P}_{\theta_0}(m^{1/4}\|f_m^*(Z) - \theta_0\|_2 > \varepsilon) \rightarrow 0,$$

for all $\varepsilon > 0$. For a bounded parameter space $\|\Theta\|_\infty < B$, this implies

$$\begin{aligned} R_{\theta_0}(f_m^*) &= \mathbb{E}_{\theta_0}[\|f_m^*(Z) - \theta_0\|_2^2] \\ &= \mathbb{E}_{\theta_0}[\|f_m^*(Z) - \theta_0\|_2^2 \mathbb{1}_{\|f_m^*(Z) - \theta_0\|_2 \leq \varepsilon/m^{1/4}}] + \mathbb{E}_{\theta_0}[\|f_m^*(Z) - \theta_0\|_2^2 \mathbb{1}_{\|f_m^*(Z) - \theta_0\|_2 > \varepsilon/m^{1/4}}] \\ &\leq \varepsilon^2/m^{1/2} + 4pB^2\mathbb{P}_{\theta_0}(m^{1/4}\|f_m^*(Z) - \theta_0\|_2 > \varepsilon) \\ &\rightarrow 0. \end{aligned}$$

For the integrated result in (16), consider

$$\lim_{m \rightarrow \infty} R(f_m^*) = \lim_{m \rightarrow \infty} \mathbb{E}_{\theta \sim \Pi} R_\theta(f_m^*).$$

Since Θ is bounded by B , the risk $R_\theta(f_m^*)$ is bounded by $4pB^2$. Furthermore, we show above that $R_\theta(f_m^*) \rightarrow 0$ for all $\theta \in \Theta$. Therefore, by the dominated convergence theorem, we have

$$\lim_{m \rightarrow \infty} R(f_m^*) = \mathbb{E}_{\theta \sim \Pi} \lim_{m \rightarrow \infty} R_\theta(f_m^*) = 0. \quad \square$$

A.2 Approximation Error

Proof of (17). For the squared loss function, and any f (such as $f_{\phi_m^*}$) we have

$$\begin{aligned} R(f) &= \mathbb{E}[\|f(Z) - \theta\|_2^2] \\ &= \mathbb{E}[\|f(Z) - \mathbb{E}[\theta|Z] + \mathbb{E}[\theta|Z] - \theta\|_2^2] \\ &= \mathbb{E}[\|f(Z) - \mathbb{E}[\theta|Z]\|_2^2 + \mathbb{E}[\mathbb{E}[\theta|Z] - \theta]^2] + \underbrace{2\mathbb{E}[\mathbb{E}[(f(Z) - \mathbb{E}[\theta|Z])(\mathbb{E}[\theta|Z] - \theta)|Z]]}_{=0} \\ &= \mathbb{E}[f(Z) - f^*(Z)]^2 + R(f_m^*). \quad \square \end{aligned}$$

Proof of Lemma 4.3. Note that the continuity of p_θ implies that of $p_{\theta,m}$. Let $B < \infty$ be such that $\Theta \subseteq [-B, B]$. Consider a point $z_0 \in \mathcal{Z}^m$ and a sequence $z_n \rightarrow z_0$, eventually contained in the domain of f . Let $K \subset \mathcal{Z}^m$ be a compact set containing z_0 and almost all z_n , and define

$$P = \sup_{\theta \in \Theta, z \in K} p_{\theta,m}(z).$$

Since p is continuous and $\Theta \times K$ is compact, P is finite. Next, let

$$q_n(\theta) = \theta \pi(\theta) p_{\theta,m}(z_n), \quad r_n(\theta) = \pi(\theta) p_{\theta,m}(z_n).$$

These functions are dominated by $BP\pi(\theta)$ and $P\pi(\theta)$, respectively, and converge pointwise to q_0 and r_0 . Hence by dominated convergence,

$$f(z_n) = \mathbb{E}(\theta|Z = z_n) = \frac{\int_{\Theta} q_n(\theta) d\theta}{\int_{\Theta} r_n(\theta) d\theta} \rightarrow \frac{\int_{\Theta} q_0(\theta) d\theta}{\int_{\Theta} r_0(\theta) d\theta} = f(z_0).$$

Note that for large n the denominator $\int_{\Theta} r_n(\theta) d\theta$ is positive, since z_n is eventually in the domain of f . Since the choice of z_0 and z_n was arbitrary, this implies that f is continuous. \square

Proof of Proposition 4.6. Fix $\varepsilon > 0$ and consider f^* to be continuous by Assumption 4.2. Let B be the bound on Θ from Assumption 3.2. Let $\varepsilon_1 = \frac{\varepsilon}{8pB^2}$ and, using Assumption 4.4, choose M such that

$$\mathbb{P}_{\theta_0}(\|Z\|_{\infty} > M) < \varepsilon_1 \quad \forall \theta_0 \in \Theta.$$

Next, let $\varepsilon_2 = \sqrt{\frac{\varepsilon}{2}}$ and, using Theorem 4.1, choose a neural network $f_{\phi_m^*}$ with

$$\sup_{z \in [-M, M]^D} \|f_{\phi_m^*}(z) - f^*(z)\|_2 < \varepsilon_2.$$

By adding another layer to this network that maps each output to the interval $[-B, B]$, we can ensure that the output of the network is bounded by B . This can be achieved using the ReLU activation function σ and the mapping

$$x \mapsto \sigma(X + B) - \sigma(X - B) - B,$$

which is the identity on $[-B, B]$ and equal to $\pm B$ elsewhere. Then, for any $\theta_0 \in \Theta$,

$$\begin{aligned} R_{\theta_0}(f_{\phi_m^*}) - R_{\theta_0}(f^*) &= \mathbb{E}_{\theta_0}[\|f_{\phi_m^*}(Z) - f_m^*(Z)\|_2^2] \\ &\leq \mathbb{P}_{\theta_0}(\|Z\|_{\infty} > M) 4pB^2 + \mathbb{P}_{\theta_0}(\|Z\|_{\infty} \leq M) \varepsilon_2^2 \\ &\leq \varepsilon_1 4pB^2 + \varepsilon_2^2 \\ &= \frac{\varepsilon}{8pB^2} 4pB^2 + \frac{\varepsilon}{2} \\ &= \varepsilon. \end{aligned}$$

Since this bound holds pointwise for all $\theta_0 \in \Theta$, we can integrate over θ_0 to obtain

$$\begin{aligned} R(f_{\phi_m^*}) - R(f_m^*) &= \mathbb{E}_{\theta_0 \sim \Pi}[R_{\theta_0}(f_{\phi_m^*}) - R_{\theta_0}(f_m^*)] \\ &\leq \mathbb{E}_{\theta_0 \sim \Pi}[\varepsilon] \\ &= \varepsilon. \end{aligned} \quad \square$$

A.3 Generalization Error

Proof of Lemma 5.3. Starting from (20), with $\delta/2$ in place of δ , we obtain with probability at least $1 - \delta/2$ that

$$\begin{aligned} |R(A_S) - R_N(A_S)| &\leq \frac{\hat{N}(S)}{N} \varepsilon + E \cdot \left(\frac{N - \hat{N}(S)}{N} + \sqrt{\frac{2K \log(2) + 2 \log(\frac{2}{\delta})}{N}} \right) \\ &\leq E \cdot \left(\frac{N - \hat{N}(S)}{N} \right) + \varepsilon + E \cdot \sqrt{\frac{2K \log(2) + 2 \log(\frac{2}{\delta})}{N}}. \end{aligned}$$

Note that the ratio $\frac{N - \hat{N}(S)}{N}$ is the proportion of (i.i.d.) samples not in $\mathcal{X}' \times \mathcal{Y}'$. Hence, we can use Hoeffding's inequality to bound this term as

$$\begin{aligned} &\mathbb{P}\left(\frac{N - \hat{N}(S)}{N} - \mathbb{P}((X, Y) \notin \mathcal{X}' \times \mathcal{Y}') > t\right) \leq \exp(-2Nt^2) \\ \Rightarrow &\mathbb{P}\left(\frac{N - \hat{N}(S)}{N} - \mathbb{P}((X, Y) \notin \mathcal{X}' \times \mathcal{Y}') > \sqrt{\frac{\log(\frac{2}{\delta})}{2N}}\right) \leq \frac{\delta}{2} \\ \Rightarrow &\mathbb{P}\left(\frac{N - \hat{N}(S)}{N} \leq \mathbb{P}((X, Y) \notin \mathcal{X}' \times \mathcal{Y}') + \sqrt{\frac{\log(\frac{2}{\delta})}{2N}}\right) \geq 1 - \frac{\delta}{2}. \end{aligned}$$

Plugging this into the above bound, and adapting the probability bound of the statement, we get with probability at least $1 - \delta$ that

$$\begin{aligned} |R(A_S) - R_N(A_S)| &\leq E \cdot \left(\mathbb{P}((X, Y) \notin \mathcal{X}' \times \mathcal{Y}') + \sqrt{\frac{\log(\frac{2}{\delta})}{2N}} \right) + \varepsilon + E \cdot \sqrt{\frac{2K \log(2) + 2 \log(\frac{2}{\delta})}{N}} \\ &= \varepsilon + E \cdot \left(\mathbb{P}((X, Y) \notin \mathcal{X}' \times \mathcal{Y}') + \sqrt{\frac{\log(\frac{2}{\delta})}{2N}} + \sqrt{\frac{2K \log(2) + 2 \log(\frac{2}{\delta})}{N}} \right). \end{aligned}$$

□

Proof of Lemma 5.4. Consider a neural network with L layers, a single output, and activation function satisfying $|\sigma(a) - \sigma(b)| \leq \beta |a - b|$. For the absolute value loss function $\ell'(y_1, y_2) = |y_1 - y_2|$, and any $x, x' \in \mathcal{X}$, $y, y' \in \mathcal{Y}$, Lemma 4 in [Xu and Mannor \[2012\]](#) then yields

$$\begin{aligned} \left| |A_s(x) - y| - |A_s(x') - y'| \right| &= |\ell'(A_s(x), y) - \ell'(A_s(x'), y')| \\ &\leq (1 + \alpha^L \beta^L) \|(x, y) - (x', y')\|_\infty. \end{aligned} \quad (27)$$

For the quadratic loss function ℓ , p -dimensional output, and the ReLU activation function used in the lemma, which implies $\beta = 1$, we have

$$\begin{aligned} |\ell(A_s(x), y) - \ell(A_s(x'), y')| &= \left| \|A_s(x) - y\|_2^2 - \|A_s(x') - y'\|_2^2 \right| \\ &\leq \sum_{i=1}^p \left| |A_s(x)_i - y_i|^2 - |A_s(x')_i - y'_i|^2 \right| \\ &\leq \sum_{i=1}^p (|A_s(x)_i - y_i| - |A_s(x')_i - y'_i|) (|A_s(x)_i - y_i| + |A_s(x')_i - y'_i|) \\ &= 4B \sum_{i=1}^p \left| |A_s(x)_i - y_i| - |A_s(x')_i - y'_i| \right| \end{aligned} \quad (28)$$

$$\begin{aligned} &\leq 4pB \max_i \left| |A_s(x)_i - y_i| - |A_s(x')_i - y'_i| \right| \\ &\leq 4pB (1 + \alpha^L) \|(x, y) - (x', y')\|_\infty. \end{aligned} \quad (29)$$

In (28) we use that \mathcal{Y} is bounded by B , and in (29) we use (27).

Setting $c(s) \equiv c = 4pB(1 + \alpha^L)$, and considering the infinity norm, Example 4 in [Xu and Mannor \[2012\]](#) implies that the neural networks are $(K(\gamma), c\gamma)$ -robust on compact sets $\mathcal{X}' \times \mathcal{Y}$ for

$$\begin{aligned} K(\gamma) &= \mathcal{N}(\gamma/2, \mathcal{X}' \times \mathcal{Y}, \|\cdot\|_\infty) \\ c &= 4pB(\alpha^L + 1). \end{aligned}$$

Furthermore, since the bound $c\gamma$ does not depend on s , the definition of pseudo-robustness is immediately satisfied, as well, for $\hat{N}(S) = \#\{i \mid (x_i, y_i) \in \mathcal{X}' \times \mathcal{Y}\}$. \square

Before proving Corollary 5.5, we establish a lemma about the term labelled ‘‘Generalization Error 2’’ in (7). Recall the notation $D = md$.

Lemma A.2. (See Proof.) *Suppose Assumptions 3.2 and 4.4 hold. Consider a fixed network architecture with L layers, let ϕ_m^* be its optimal weights with respect to risk R , and let $\phi_m^{N, \alpha(N)}$ be the restricted empirical risk minimizer defined in (23). Assume that the output of the network ϕ_m^* is bounded by the same B as in (21) and Assumption 3.2. Then there exists $\zeta_1(\delta, N)$ that converges to zero as N grows, and $\alpha(N)$, such that for every $\delta \in (0, 1)$, with probability at least $1 - \delta$,*

$$R(\phi_m^{N, \alpha(N)}) - R_N(\phi_m^{N, \alpha(N)}) < \zeta_1(\delta, N).$$

An expression for $\zeta_1(\delta, N)$ is given in the proof.

Proof of Lemma A.2. For $M < \infty$ let $\mathcal{X}' = [-M, M]^D \cap \mathcal{X} \subseteq \mathcal{X}$. By Assumption 3.2, the output space \mathcal{Y} is bounded by B . Hence, a uniformly spaced covering with hyperrectangles yields

$$\mathcal{N}(\gamma/2, \mathcal{X}' \times \mathcal{Y}, \|\cdot\|_\infty) \leq \left\lceil \frac{2B}{\gamma} \right\rceil^p \left\lceil \frac{2M}{\gamma} \right\rceil^D.$$

Recall that for p -dimensional outputs bounded by B , the quadratic loss is bounded by $E = 4pB^2$. Using the statements and notation of Lemmas 5.3 and 5.4 we have with probability $1 - \delta$ that

$$R(\phi_m^N) - R_N(\phi_m^N) \leq \varepsilon + E \cdot \left(\mathbb{P}(\|Z\|_\infty > M) + \sqrt{\frac{\log(\frac{2}{\delta})}{2N}} + \sqrt{\frac{2K \log(2) + 2 \log(\frac{2}{\delta})}{N}} \right)$$

$$= 4pB(\alpha^L + 1)\gamma \tag{30}$$

$$+ 4pB^2 \mathbb{P}(\|Z\|_\infty > M) \tag{31}$$

$$+ 4pB^2 \sqrt{\frac{\log(\frac{2}{\delta})}{2N}} \tag{32}$$

$$+ 4pB^2 \sqrt{\frac{2 \left\lceil \frac{2B}{\gamma} \right\rceil^p \left\lceil \frac{2M}{\gamma} \right\rceil^D \log(2) + 2 \log(\frac{2}{\delta})}{N}}. \tag{33}$$

In (31), we use the fact that the probability $\mathbb{P}((X, Y) \notin \mathcal{X}' \times \mathcal{Y}')$ can be rewritten as $\mathbb{P}(\|Z\|_\infty > M)$, where the probability is taken with respect to both the prior distribution $\theta \sim \Pi$ and the data distribution $Z \sim p_\theta$. For this sum to converge to zero, we let α , γ , and M be functions of N . To this end, fix $0 < \xi < \frac{1}{D+p}$ and $0 < \kappa < \frac{1-2\xi}{D+p} - \xi$, and set

$$\begin{aligned} M(N) &= N^{\frac{1-2\xi}{D+p} - \xi - \kappa}, \\ \gamma(N) &= N^{-\xi - \kappa}, \\ \alpha(N) &= N^{\frac{\xi}{L}}. \end{aligned} \tag{34}$$

Note that $M(N) \rightarrow \infty$ for $N \rightarrow \infty$, and hence by the assumption of a uniformly tight model in Assumption 4.4, term (31) goes to zero. Apart from N itself, all expressions in (32) are constant w.r.t. N , and hence this term goes to zero as well.

For (30), we have

$$\begin{aligned} 4pB(\alpha(N)^L + 1)\gamma(N) &= 4pB(N^\kappa + 1)N^{-\xi-\kappa} \\ &= 4pB(1 + N^{-\kappa})N^{-\xi} \rightarrow 0. \end{aligned}$$

For (33), we observe that, for large N , $M(N)$ will be larger than B , so we have

$$\begin{aligned} 2\left(\frac{2B}{\gamma(N)}\right)^p \left(\frac{2M(N)}{\gamma(N)}\right)^D N^{-1} &\leq 2\left(\frac{2M(N)}{\gamma(N)}\right)^{D+p} N^{-1} \\ &= 2^{D+p+1} \left(\frac{N^{\frac{1-2\xi}{D+p} - \xi - \kappa}}{N^{-\xi - \kappa}}\right)^{D+p} N^{-1} \\ &= 2^{D+p+1} N^{-2\xi} \\ &\rightarrow 0. \end{aligned} \tag{35}$$

Up to some vanishing noise introduced by the ceiling operation $\lceil \cdot \rceil$, expression (33) is a monotone transformation of this term, and also converges to zero.

The expression for $\zeta_1(\delta, N)$ is then given by the sum of the terms in (30) to (33), replacing M , γ , and α by their respective functions of N . \square

Proof of Corollary 5.5. We have the decomposition as in (7)

$$R(\phi_m^{N,\alpha(N)}) - R(\phi_m^*) = R(\phi_m^{N,\alpha(N)}) - R_N(\phi_m^{N,\alpha(N)}) \tag{36}$$

$$+ R_N(\phi_m^{N,\alpha(N)}) - R_N(\phi_m^*) \tag{37}$$

$$+ R_N(\phi_m^*) - R(\phi_m^*). \tag{38}$$

Using the rates defined in (34), the term on the right-hand side of (36) satisfies with probability at least $1 - \delta/2$ that

$$R(\phi_m^{N,\alpha(N)}) - R_N(\phi_m^{N,\alpha(N)}) < \zeta_1(\delta/2, N).$$

To bound (37), let N_1 be such that $\phi_m^* \in \Phi^{\alpha(N),L}$ for all $N \geq N_1$; such an N_1 exists since $\alpha(N) \rightarrow \infty$ as $N \rightarrow \infty$. For these $N \geq N_1$ the parametrization ϕ_m^* is a candidate for the empirical risk minimizer $\phi_m^{N,\alpha(N)}$ and hence

$$R_N(\phi_m^{N,\alpha(N)}) - R_N(\phi_m^*) \leq 0.$$

Lastly, for (38), observe that $R_N(\phi_m^*)$ is a finite sample approximation of $R(\phi_m^*)$, and hence we can use Hoeffding's inequality to bound the difference.

$$\begin{aligned} \mathbb{P}(R_N(\phi_m^*) - R(\phi_m^*) > \lambda) &= \mathbb{P}\left(N^{-1} \sum_{i=1}^N \ell(\phi_m^*(Z_i), Y_i) - \mathbb{E}[\ell(\phi_m^*(Z), Y)] > \lambda\right) \\ &\leq \exp\left(-\frac{N\lambda^2}{8p^2B^4}\right). \end{aligned} \tag{39}$$

Setting $\lambda = pB^2 \sqrt{\frac{8 \log(\frac{2}{\delta})}{N}}$, we obtain with probability at least $1 - \delta/2$ that

$$R_N(\phi_m^*) - R(\phi_m^*) < pB^2 \sqrt{\frac{8 \log(\frac{2}{\delta})}{N}} =: \zeta_2(\delta/2, N).$$

Note that $\zeta_2(\delta, N) \rightarrow 0$ for $N \rightarrow \infty$. Putting everything together, we have for all $N \geq N_1$ with probability at least $1 - \delta$ that

$$R(\phi_m^{N, \alpha(N)}) - R(\phi_m^*) < \zeta_1(\delta/2, N) + \zeta_2(\delta/2, N) =: \zeta(\delta, N).$$

Since $\zeta(\delta, N)$ is the sum of two converging sequences, it also converges to zero for $N \rightarrow \infty$. \square

A.4 Joint Result

Proof of Theorem 6.1. Recall the error decomposition (6):

$$R(\phi_m^N) = \underbrace{R(f_m^*)}_{\text{Bayes Risk}} + \underbrace{R(\phi_m^*) - R(f_m^*)}_{\text{Approximation Error}} + \underbrace{R(\phi_m^N) - R(\phi_m^*)}_{\text{Generalization Error}}.$$

For $m \in \mathbb{N}$, let $\varepsilon_m = R(f_m^*)$ and, using Proposition 4.6, choose ϕ_m^* such that

$$R(\phi_m^*) - R(f_m^*) \leq \varepsilon_m. \quad (40)$$

This ϕ_m^* satisfies the conditions of Corollary 5.5, so we can, with N_1 and ζ from the Corollary, choose $N(m)$ satisfying $N(m) \geq N_1$ and

$$\zeta(3\varepsilon_m, N(m)) \leq \varepsilon_m. \quad (41)$$

Putting these bounds together, we have with probability at least $1 - 3\varepsilon_m$ that

$$\begin{aligned} R(\phi_m^{N(m), \alpha(m)}) &= R(f_m^*) + (R(\phi_m^*) - R(f_m^*)) + (R(\phi_m^{N(m), \alpha(m)}) - R(\phi_m^*)) \\ &\leq \varepsilon_m + \varepsilon_m + \varepsilon_m = 3\varepsilon_m. \end{aligned}$$

By Corollary 3.3, the term ε_m converges to zero as $m \rightarrow \infty$.

To show that $R(\phi_m^{N(m), \alpha(m)})$ converges to zero in probability, consider a fixed $\varepsilon > 0$, and choose M such that $3\varepsilon_m < \varepsilon$ for all $m \geq M$. This yields

$$\mathbb{P}(R(\phi_m^{N(m), \alpha(m)}) > \varepsilon) \leq \mathbb{P}(R(\phi_m^{N(m), \alpha(m)}) > 3\varepsilon_m) \leq 3\varepsilon_m \leq \varepsilon, \quad \forall m \geq M,$$

which implies

$$R(\phi_m^{N(m), \alpha(m)}) \xrightarrow{P} 0 \quad \text{as } m \rightarrow \infty. \quad \square$$

Proof of Corollary 6.2. In this proof, we repeatedly make use of the fact that for uniformly bounded random variables $0 \leq |X_m| < B < \infty$, convergence in probability and convergence in r -th mean are equivalent, i.e.,

$$X_m \xrightarrow{P} 0 \iff X_m \xrightarrow{L^r} 0.$$

Recall that the parameter space Θ is bounded by some $B < \infty$, and we constructed ϕ_m such that its output is also bounded by B . The quadratic loss function $\ell(\theta, \hat{\theta}) = (\theta - \hat{\theta})^2$ is therefore nonnegative and bounded by $E = 4pB^2$. Recall that the risk R is the expectation of the loss function, conditioned on the training sample S_m . Consequently, the risk $R(\phi_m(Z))$ is bounded by E as well.

Next, note that the convergence stated in Theorem 6.1 is equivalent to the convergence of $R(\phi_m)$ to zero in probability. Hence, we also have convergence in mean, implying

$$\begin{aligned} &R(\phi_m) \xrightarrow{L^1} 0 \\ \Rightarrow &\mathbb{E}(\mathbb{E}(\ell(\theta, f_{\phi_m}(Z)) \mid S_m)) \longrightarrow 0 \\ &\Rightarrow \mathbb{E}(\ell(\theta, f_{\phi_m}(Z))) \longrightarrow 0 \\ &\Rightarrow \mathbb{E}((\theta - f_{\phi_m}(Z))^2) \longrightarrow 0 \\ &\Rightarrow f_{\phi_m}(Z) \xrightarrow{L^2} \theta, \end{aligned} \quad (42)$$

which in turn implies $f_{\phi_m}(Z) \xrightarrow{p} \theta$, completing the proof of the first two expressions in the corollary.

Regarding the pointwise risk, recall that $R_\theta(\phi_m) = \mathbb{E}(\ell(\theta, f_{\phi_m}(Z)) \mid S_m, \theta)$, which is a random variable with respect to the distribution of S_m, θ . Starting with the convergence in (42), we have

$$\begin{aligned} &\Rightarrow \mathbb{E}(\ell(\theta, f_{\phi_m}(Z))) \longrightarrow 0 \\ \Rightarrow &\mathbb{E}(\mathbb{E}(\ell(\theta, f_{\phi_m}(Z)) \mid S_m, \theta)) \longrightarrow 0 \\ &\Rightarrow R_\theta(\phi_m) \xrightarrow{L^1} 0, \end{aligned}$$

which is again equivalent to convergence in probability, completing the proof. \square

A.5 Rate Discussion

A.5.1 Setup

Theorem 6.1 guarantees the existence of a sequence $N(m)$ that ensures convergence of the generalization error to zero at the desired rate. In the following, we analyze how the convergence rate depends on N and derive a lower bound on $N(m)$ sufficient to guarantee this convergence.

In the proof of Lemma A.2, the generalization error is decomposed into the terms (30), (31), (32), and (33), whose joint convergence to zero is guaranteed by the choices of $M(N)$, $\gamma(N)$, and $\alpha(N)$ in (34), which depend on suitably chosen constants κ and ξ . In order to investigate the required growth rate of $N(m)$, we first define these values κ and ξ as functions of m :

$$\xi(m) = \frac{1}{2(md+p)}, \quad \kappa(m) = \frac{1 - \frac{2}{(md+p)}}{4(md+p)}. \quad (43)$$

These values are chosen as the midpoint of their admissible ranges, respectively, different choices would yield similar rates to the ones discussed below. Note that for large m , the value of $\kappa(m)$ is asymptotically equivalent to $\frac{1}{4(md+p)}$.

We recall the decomposition (7) and note that its second term can be dropped since it is almost surely negative. The third term in this decomposition can be bounded by Hoeffding's inequality as in (39), and a sufficient condition for the training sample size is that $N(m)$ grows faster than ε_m^{-2} as $m \rightarrow \infty$, which is a much weaker condition than the ones derived below.

A.5.2 Generalization Error

Firstly, for (35), and hence (33), to converge to zero, we need to choose $N(m)$ such that

$$2^{md+p} N(m)^{-2\xi(m)} \rightarrow 0,$$

implying superexponential growth in m . In order to obtain convergence at a certain rate ε_m , for example at the same rate as the Bayes risk, we choose

$$N(m) \geq \left(\frac{1}{\varepsilon_m}\right)^{md+p} \exp((\log 2)(md+p)^2). \quad (44)$$

The two remaining terms (30) and (32) then converge to zero faster than (33). Convergence of (31) is guaranteed by the choice of M , the rate will be discussed below.

A.5.3 Network Complexity

In order to apply the error decomposition in the proof of Corollary 5.5, the optimal network ϕ_m^* must be in the set of considered networks, i.e., $\phi_m^* \in \Phi^{\alpha(m), L}$. To get a first insight into the growth of $N(m)$ required to ensure this, we consider the mild assumption that the threshold $\alpha(m)$ needs to diverge to infinity as $m \rightarrow \infty$. Applying logarithms to the definition of α in (34), we then obtain

$$\frac{\kappa(m)}{L} \log(N(m)) \rightarrow \infty. \quad (45)$$

Keeping the number of layers L fixed, as is the case for the shallow networks considered in this paper, and plugging in $\kappa(m) \approx \frac{1}{4(md+p)}$, this implies that $\log(N(m))$ must grow faster than linearly in m , or equivalently, $N(m)$ must grow faster than exponentially in m . Concretely,

$$N(m) \in \omega(\exp(4(md+p)L)),$$

where the notation $u(m) \in \omega(v(m))$ means that $u(m)/v(m) \rightarrow \infty$ as $m \rightarrow \infty$, which is already satisfied by the growth rate implied by (44).

However, a more realistic assumption on the network complexity is that the number of nodes in the optimal network ϕ_m^* grows both in the input dimension m and the required approximation accuracy ε_m , for example as $\exp(g(m, \varepsilon_m))$ for some function $g(m, \varepsilon)$. Assuming that the average magnitudes of the optimal network weights stay constant, $\alpha(m)$ must also satisfy

$$\begin{aligned} \alpha(m) &= N(m)^{\frac{\kappa(m)}{L}} \geq \exp(g(m, \varepsilon_m)) \\ \Rightarrow \quad N(m) &\in \Omega(\exp(g(m, \varepsilon_m)4(md+p)L)), \end{aligned}$$

where the notation $u(m) \in \Omega(v(m))$ means that $u(m)/v(m)$ is bounded away from zero as $m \rightarrow \infty$. Considering the shallow networks used in this paper and some mild assumptions on the regularity of the target function f_m^* , the rate $g(m, \varepsilon_m)$ can be linear in $m \log(\varepsilon_m^{-1})$ [Yarotsky, 2017], exceeding the growth rate implied by (44). Whether it is possible to construct more efficient network architectures for multiple replicates remains an open question. From a practical standpoint, [Sainsbury-Dale et al., 2023] propose an estimator that mitigates the complexity growth with m to some extent.

A.5.4 Tail Probability

Finally, the overall bound on the generalization error also involves the convergence rate of the tail term $\mathbb{P}(\|Z\|_\infty > M)$ in (31), which is model-dependent. With the choice of $\xi(m)$ and $\kappa(m)$ from (43), the threshold M can be expressed as

$$M(m) = N(m)^{\frac{1-2\xi(m)}{md+p} - \xi(m) - \kappa(m)} = N(m)^{\kappa(m)},$$

since $\kappa(m)$ was chosen as exactly half of the remaining terms in the exponent. For distributions with sub-Gaussian tails, the probability of exceeding this threshold decays at least exponentially in $M(m)^2 = N(m)^{2\kappa(m)}$. To obtain rate ε_m in this case it is necessary that

$$N(m) \in \Omega\left(\log(\varepsilon_m^{-1})^{2(md+p)}\right).$$

In contrast, for heavy-tailed distributions such as those with Fréchet margins, the decay of (31) is merely polynomial in $M(m)$, leading to

$$N(m) \in \Omega\left((\varepsilon_m^{-1})^{C(md+p)}\right),$$

for a constant $C > 0$ in order to obtain decrease at rate ε_m .

B Proofs of applicability to examples

B.1 Multivariate normal distribution

Below, let $\|\Sigma\|_\infty$ denote the element-wise (absolute) maximum of a matrix Σ .

Lemma B.1. *Let Σ_θ be a parametric covariance matrix, satisfying for all $\varepsilon > 0$*

$$\inf_{\substack{\theta \in \Theta \\ \|\theta - \theta_0\| \geq \varepsilon}} \|\Sigma_\theta - \Sigma_{\theta_0}\|_\infty =: I_\varepsilon > 0 \quad (46)$$

$$\sup_{\theta \in \Theta} \|\Sigma_\theta\|_\infty =: S < \infty. \quad (47)$$

Let $\hat{\Sigma}$ be the empirical covariance matrix. For $\delta = I_\varepsilon/2$, define the tests

$$\phi_m^\varepsilon = \begin{cases} 0 & \text{if } \|\hat{\Sigma} - \Sigma_{\theta_0}\|_\infty \leq \delta \\ 1 & \text{else.} \end{cases}$$

Then the tests satisfy

$$\begin{aligned} \mathbb{E}_{\theta_0}(\phi_m^\varepsilon) &\rightarrow 0 \quad \text{for } m \rightarrow \infty, \\ \sup_{\|\theta - \theta_0\| \geq \varepsilon} \mathbb{E}_\theta(1 - \phi_m^\varepsilon) &\rightarrow 0 \quad \text{for } m \rightarrow \infty. \end{aligned}$$

Proof of Lemma B.1. Since, under θ_0 , $\hat{\Sigma}$ is a consistent estimator of Σ_{θ_0} , and $\delta > 0$, we have

$$\mathbb{E}_{\theta_0}(\phi_m^\varepsilon) = \mathbb{P}_{\theta_0}(\|\hat{\Sigma} - \Sigma_{\theta_0}\|_\infty > \delta) \rightarrow 0.$$

Furthermore, for $\|\theta - \theta_0\| \geq \varepsilon$, let i_θ, j_θ be the index of the maximum element of $|\Sigma_\theta - \Sigma_{\theta_0}|$. This index satisfies $|\Sigma_{\theta, i_\theta j_\theta} - \Sigma_{\theta_0, i_\theta j_\theta}| \geq I_\varepsilon$. Then

$$\begin{aligned} \mathbb{E}_\theta(1 - \phi_m^\varepsilon) &= \mathbb{P}_\theta(\|\hat{\Sigma} - \Sigma_{\theta_0}\|_\infty \leq \delta) \\ &\leq \mathbb{P}_\theta(|\hat{\Sigma}_{i_\theta j_\theta} - \Sigma_{\theta_0, i_\theta j_\theta}| \leq \delta) \\ &\leq \mathbb{P}_\theta(|\Sigma_{\theta, i_\theta j_\theta} - \Sigma_{\theta_0, i_\theta j_\theta}| - |\hat{\Sigma}_{i_\theta j_\theta} - \Sigma_{\theta, i_\theta j_\theta}| \leq \delta) \\ &\leq \mathbb{P}_\theta(I_\varepsilon - |\hat{\Sigma}_{i_\theta j_\theta} - \Sigma_{\theta, i_\theta j_\theta}| \leq \delta) \\ &= \mathbb{P}_\theta(|\hat{\Sigma}_{i_\theta j_\theta} - \Sigma_{\theta, i_\theta j_\theta}| \geq I_\varepsilon - \delta) \end{aligned}$$

Since $\delta = I_\varepsilon/2$, the last threshold simplifies to $I_\varepsilon - \delta = \delta$. To bound this probability, observe that for any entry i, j of the empirical covariance matrix, we have (using [Anderson, 2003, Theorem 3.3.2] and well-known properties of the chi-squared distribution)

$$\text{Var}_\theta(\hat{\Sigma}_{ij}) \leq \frac{2\|\Sigma_\theta\|_\infty^2}{m-1} \leq \frac{2S^2}{m-1}$$

and hence by Chebyshev's inequality and the fact that $\hat{\Sigma}$ is unbiased,

$$\mathbb{P}_\theta(|\hat{\Sigma}_{ij} - \Sigma_{\theta, ij}| \geq \delta) \leq \frac{\text{Var}_\theta(\hat{\Sigma}_{ij})}{\delta^2} \leq \frac{2S^2}{(m-1)\delta^2}.$$

In particular, this holds for $i, j = i_\theta, j_\theta$. Since the bound is independent of θ , we have

$$\sup_{\|\theta - \theta_0\| \geq \varepsilon} \mathbb{E}_\theta(1 - \phi_m^\varepsilon) \leq \frac{2S^2}{(m-1)\delta^2} \rightarrow 0, \quad \text{for } m \rightarrow \infty. \quad \square$$

B.2 Gaussian processes

Below, we consider a fixed set of points x_1, \dots, x_d at which the Gaussian processes are observed and denote

$$\begin{aligned} H_h &= \{(i, j) \mid \|x_i - x_j\| = h\}, \\ H &= \{h \mid H_h \neq \emptyset\}. \end{aligned}$$

For a parametric covariance function $C_\theta(h)$, denote

$$\Sigma_\theta = (C_\theta(\|x_i - x_j\|))_{ij}.$$

Lemma B.2. *Recall the (powered) exponential model from (8) with parameter vector $\theta = (\tau, \lambda, \alpha)$ and covariance function*

$$C_\theta(h) = \exp(-(h/\lambda)^\alpha) + \tau^2 \mathbb{1}_{h=0}.$$

Let τ be bounded by some $\tau_1 < \infty$. For $|H| \geq 3$, the powered exponential model satisfies the conditions of Lemma B.1. If $\alpha > 0$ is fixed and omitted from the parameter vector θ , the conditions are already satisfied for $|H| \geq 2$.

Proof of Lemma B.2. Note that (47) is satisfied in both scenarios because by positive definiteness of the covariance function, we have

$$\sup_{\theta \in \Theta} \|\Sigma_\theta\|_\infty \leq \sup_{\theta \in \Theta} C_\theta(0) = 1 + \tau_1^2 < \infty.$$

For the powered exponential model, denote $\theta = (\tau, \lambda, \alpha)$, choose some distinct, non-zero $h_1, h_2 \in H$, and define the function $f : \mathbb{R}^3 \rightarrow \mathbb{R}^3$ with

$$f(\tau, \lambda, \alpha) = (C_\theta(0), C_\theta(h_1), C_\theta(h_2)).$$

If we can show that this function has a continuous inverse f^{-1} , condition (46) is satisfied, because then for every $y_0 \in \mathbb{R}^3$ and $\varepsilon > 0$, there is some $\delta > 0$ such that for all $y \in \mathbb{R}^3$ we have

$$\begin{aligned} \|y - y_0\| < \delta &\Rightarrow \|f^{-1}(y) - f^{-1}(y_0)\| < \varepsilon \\ \therefore \|f^{-1}(y) - f^{-1}(y_0)\| > \varepsilon &\Rightarrow \|y - y_0\| > \delta \\ &\therefore \|x - x_0\| > \varepsilon \Rightarrow \|f(x) - f(x_0)\| > \delta \\ \therefore \inf_{\|x - x_0\| > \varepsilon} \|f(x) - f(x_0)\| &\geq \delta. \end{aligned} \tag{48}$$

To do so, observe that f^{-1} can be expressed coordinatewise by

$$\begin{aligned} \tau &= \sqrt{C_\theta(0) - 1} \\ \alpha &= \frac{\log(-\log C_\theta(h_1)) - \log(-\log C_\theta(h_2))}{\log h_1 - \log h_2} \\ \lambda &= \frac{h_1}{(-\log C_\theta(h_1))^{1/\alpha}}. \end{aligned}$$

Each of these are continuous functions, and hence f^{-1} is continuous as well.

For the fixed α case, the same argument applies with

$$f(\tau, \lambda) = (C_\theta(0), C_\theta(h_1))$$

and the inverse defined coordinatewise as above, plugging in the fixed α in the expression for λ . \square

Lemma B.3. Recall the Matérn model from (9), with fixed smoothness ν and parameter vector $\theta = (\tau, \lambda)$.

$$C_\theta(h) = \frac{2^{1-\nu}}{\Gamma(\nu)} \left(\sqrt{2\nu} \frac{h}{\lambda} \right)^\nu K_\nu \left(\sqrt{2\nu} \frac{h}{\lambda} \right) + \tau^2 \mathbb{1}_{h=0},$$

Let τ be bounded by some $\tau_1 < \infty$. For $|H| \geq 2$, this model satisfies the conditions of Lemma B.1.

Proof of Lemma B.3. The value of the Matérn covariance function at $h = 0$ is

$$C_\theta(0) = 1 + \tau^2.$$

Hence, (47) is satisfied because by positive definiteness of the covariance function, we have

$$\sup_{\theta \in \Theta} \|\Sigma_\theta\|_\infty \leq \sup_{\theta \in \Theta} C_\theta(0) = 1 + \tau_1^2 < \infty.$$

For $x > 0$, the function $x \mapsto x^\nu K_\nu(x)$ is strictly decreasing and continuous [Zhang et al., 2023, Proposition E.2]. Hence, for fixed $0 < h \in H$, the function $\lambda \mapsto C_\theta(h)$ is strictly increasing and continuous, and so is its inverse. Therefore, the map

$$f(\tau, \lambda) = (C_\theta(0), C_\theta(h))$$

has a continuous inverse f^{-1} , and by the same argument as in (48), it follows that (46) is satisfied for the Matérn model. \square

Lemma B.4. Both the powered exponential and Matérn covariance functions are differentiable in quadratic mean with non-singular Fisher information matrix.

Proof of Lemma B.4. Lemma 7.6 and Example 7.7 in van der Vaart [1998] state that the density of an exponential family

$$p_\theta(x) = d(\theta)h(x) \exp(Q(\theta)^\top t(x))$$

is differentiable in quadratic mean if the maps $\theta \mapsto Q(\theta)$ are continuously differentiable and map the parameter space Θ into the interior of the natural parameter space.

In the case of Gaussian distributions with fixed mean, the entries of $Q(\theta)$ correspond to the entries of the precision matrix Σ_θ^{-1} . Since both the powered exponential and Matérn covariance functions are strictly positive definite [Stein, 2012], the precision matrix is non-singular, and hence in the interior of the natural parameter space. Since matrix inversion is a continuous operation, it remains to show that the covariance functions, evaluated at fixed distances $h \in H$, are continuously differentiable in θ .

For the powered exponential model from (8), this is immediately clear. For the Matérn model from (9) with fixed smoothness ν , this follows from the fact that $x \mapsto x^\nu K_\nu(x)$ is continuously differentiable [Zhang et al., 2023, e.g., proof of Proposition E.2]. \square

Proof of Lemma 3.4. By Lemmas B.2 and B.3, we can construct the required tests, and by Lemma B.4, both models are differentiable in quadratic mean with non-singular Fisher information matrix. The condition on the prior can be satisfied for a compact parameter space Θ , for example by choosing the uniform distribution. \square

Proof of Lemma 4.8. To check Assumption 4.4, observe that the variance of the powered exponential and Matérn covariance functions with bounded τ is bounded by $S = 1 + \tau_1^2$. Furthermore, recall that the mean function is assumed to be zero. Hence, for $\varepsilon > 0$ we

can choose $M = \sqrt{S}\Phi^{-1}(1 - \varepsilon/(2d))$, where Φ denotes the standard normal distribution function. Then

$$\begin{aligned}\mathbb{P}(|Z_i| > M) &\leq \Phi(-M/\sqrt{S}) + 1 - \Phi(M/\sqrt{S}) \\ &= 2(1 - \Phi(M/\sqrt{S})) \\ &= 2(1 - (1 - \varepsilon/(2d))) \\ &= \varepsilon/d,\end{aligned}$$

and hence

$$\mathbb{P}(\|Z\|_\infty > M) \leq d\mathbb{P}(|Z_i| > M) \leq \varepsilon.$$

To show continuity of the Bayes estimator (Assumption 4.2), note that the density of a centered Gaussian distribution

$$p_\theta(z) = \frac{1}{(2\pi)^{d/2}\sqrt{|\Sigma_\theta|}} \exp(-\frac{1}{2}z^\top \Sigma_\theta^{-1}z)$$

is always continuous in z and continuous in θ if the covariance matrix Σ_θ is continuous in θ . For the powered exponential and Matérn models, the covariance functions are continuous in θ , as discussed in the proof of Lemma B.4. Hence, by Lemma 4.3, the Bayes estimator is continuous for the considered models and compact parameter spaces. \square

B.3 Max-stable processes

Proof of Lemma 3.5. The applicability of the Bernstein–von Mises Theorem to the considered extreme value models is shown in Proposition 3 and Corollary 2 of [Dombry et al. \[2017b\]](#). \square

Proof of Lemma 4.9. To check Assumption 4.4, recall that we consider models with unit Fréchet margins, independent of the parameter. These margins satisfy $Z_i > 0$ almost surely, so we only need to consider the probability of the event $Z_i > M$. Let F denote the Fréchet distribution function, F^{-1} its quantile function, and for $\varepsilon > 0$ choose $M = F^{-1}(1 - \varepsilon/d)$. Then

$$\mathbb{P}(\|Z\|_\infty > M) \leq \sum_{i=1}^d \mathbb{P}(Z_i > M) = d(1 - F(M)) = \varepsilon.$$

Assumption 4.2 is checked using [Dombry et al. \[2017a\]](#). Their equation (1) gives an explicit expression for the probability density function of a max-stable distribution. Given Condition A2 from Proposition 3.2 in their paper, this expression is continuous in θ and z . In turn, Condition A2 is satisfied for the considered models, as shown in Lemma B.1 (logistic), the proof of Proposition 4.5 (Brown–Resnick), and Lemma B.3 together with the proof of Proposition 3.3 (Schlather). By Lemma 4.3, the continuity of the density in θ and z combined with the compact parameter space Θ implies that the Bayes estimator is continuous in z . \square

C Simulation study for the linear model

We consider the example of the linear model as an illustrative example, since in this case we can compute all error terms explicitly. Let $(\Omega, \mathcal{A}, \mathbb{P})$ denote a probability space. Define $Z := (Z^1, \dots, Z^m)$ such that Z^1, \dots, Z^m are independently and identically distributed random variables following a normal distribution with mean $\theta \in \Theta = \mathbb{R}$ and fixed variance σ^2 .

The distribution Π of the parameter θ is normal with mean μ and variance γ^2 . The neural estimator for estimating θ from Z is constructed using a linear model with $k \leq m$ non-zero coefficients and one intercept; this corresponds to a simple neural network with no hidden layers. The training dataset consist of N i.i.d. observations $((Z_i^1, \dots, Z_i^m), \theta_i)$, for $i = 1, \dots, N$, drawn from the joint distribution

$$\mathbb{P}(Z \in A, \theta \in B) = \int_B \int_A \frac{1}{\sqrt{(2\pi\sigma^2)^m}} \exp - \frac{\sum_{j=1}^m (z_j - \theta)^2}{2\sigma^2} \frac{1}{\sqrt{2\pi\gamma^2}} \exp - \frac{(\theta - \mu)^2}{2\gamma^2} d(z_1, \dots, z_m) d\theta,$$

where $A \in \mathcal{B}(\mathbb{R}^m)$ and $B \in \mathcal{B}(\Theta)$. The empirical risk minimization (2) simplifies in this case to

$$\min_{A_1, \dots, A_m, b} \frac{1}{N} \sum_{i=1}^N \left(\sum_{j=1}^m A_j Z_i^j + b - \theta_i \right)^2 \quad \text{s.t. } \|A\|_0 \leq k. \quad (49)$$

As N tends to infinity, this problem converges almost surely to minimization problem of the population risk, that is,

$$\min_{A_1, \dots, A_m, b} \mathbb{E} \left[\left(\sum_{j=1}^m A_j Z^j + b - \theta \right)^2 \right] \quad \text{s.t. } \|A\|_0 \leq k. \quad (50)$$

When $k = m$, the solution of (50) corresponds to the Bayes estimator $f_m^*(z) = \mathbb{E}[\theta | Z = z]$, which is a linear model with optimal parameter vector ϕ_m^* with components

$$A_1^* = \dots = A_m^* = \frac{\gamma^2}{m\gamma^2 + \sigma^2}, \quad b^* = \mu \frac{\sigma^2}{m\gamma^2 + \sigma^2},$$

whose dimension and value depend on m . The solution depends on the prior distribution of θ , the variance of Z , and the number of replicates m . Notably, the Bayes estimator differs from the maximum likelihood estimator as it is biased towards the prior assumptions. As m and γ^2 increase or σ^2 decreases, the prior assumptions become less influential, causing the Bayes estimator to approach the maximum likelihood estimator.

While the optimization problem (50) aims to minimize the expected risk $\mathbb{E}[R_\theta(\phi_m^*)]$, we can explicitly determine the pointwise risk of the estimator in this case

$$R_\theta(\phi_m^*) = (\mu - \theta)^2 \frac{\sigma^4}{(m\gamma^2 + \sigma^2)^2} + \frac{m\sigma^2\gamma^4}{(m\gamma^2 + \sigma^2)^2}.$$

When $k < m$, the solution of problem (50) does not correspond to the Bayes estimator. Instead, we have

$$R(\phi_m^*) - R(f_m^*) = \frac{\gamma^2\sigma^4 + k\sigma^2\gamma^4}{(k\gamma^2 + \sigma^2)^2} - \frac{\gamma^2\sigma^4 + m\sigma^2\gamma^4}{(m\gamma^2 + \sigma^2)^2} > 0. \quad (51)$$

The optimal risk $R(\phi^*)$ as a function of the number of active parameters k is shown in Figure 8. We clearly see how the expressiveness of the approximating function class, here measured as the number of non-zero coefficients k in a linear model, governs the approximation error. In fact, for a constant $k = 10$ this error does not vanish for growing m .

In the following, we analyze the error decomposition (7) and assume that $k = m$, that is, the optimal neural estimator is the Bayes estimator and there is no approximation error. The theoretical analysis suggests that the trained estimator is close to the true estimator when N increases exponentially in the number of replica m . Figure 9 illustrates this for $N = 100$ and $N = 1000$. While $N = 100$ is a sufficiently large training sample size for smaller m , there is a gap between the optimal neural estimator and the trained neural estimator for larger m . This gap becomes smaller when N increases.

Figure 10 shows the improvement of the neural estimator as a function of the training sample size. Here, the number of replica $m = 30$ is fixed. While for low N , the neural estimator has a large generalization error, the empirical and true risk converge to the Bayes risk in exponential dependency of N .

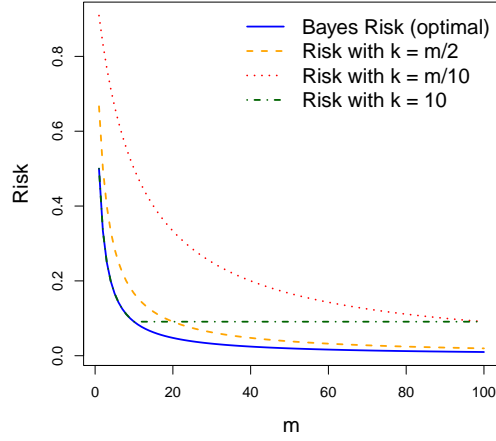


Figure 8: Bayes risk compared to the risks of different approximating functions corresponding to different choices of model complexity k , as a function of sample size m .

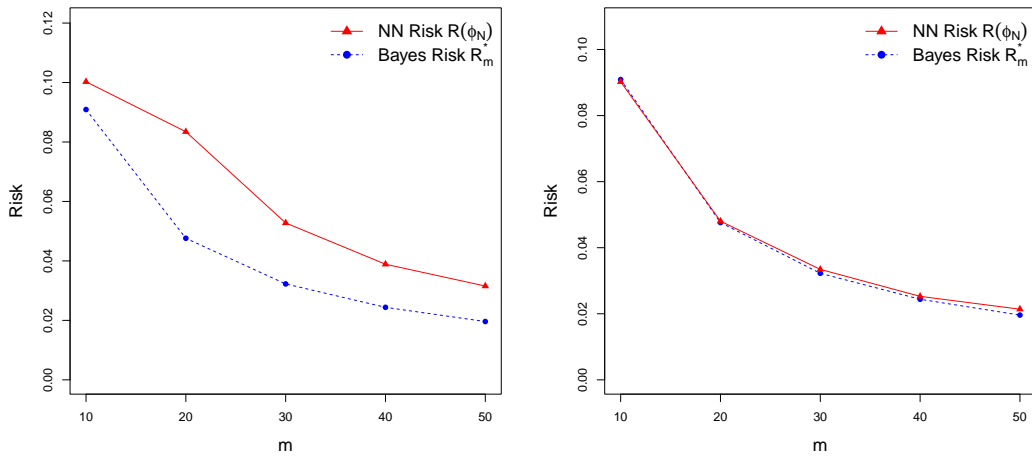


Figure 9: Bayes risk compared to the risk of the empirical risk minimizer as a function of number of replicates m , left: $N = 100$, right: $N = 1000$.

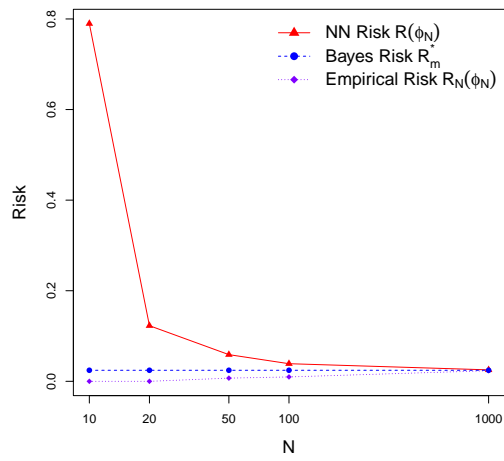


Figure 10: Generalization error for $m = 40$, logarithmically in the training data size N .

D Symbols

$\theta \in \Theta \subseteq \mathbb{R}^p$	Parameter value
$\theta_0 \in \Theta$	True parameter
Π	Prior distribution of θ
$\pi : \mathbb{R}^p \rightarrow \mathbb{R}$	Density of Π
$\{\mathcal{P}_\theta\}_{\theta \in \Theta}$	Family of distributions
$\mathcal{Z} \subseteq \mathbb{R}^d$	Codomain of each \mathcal{P}_θ
$p_\theta : \mathbb{R}^d \rightarrow \mathbb{R}$	Density of \mathcal{P}_θ
$m \in \mathbb{N}$	Number of simultaneous samples
$Z = (Z^1, \dots, Z^m)$	m -Sample (random variable)
$\mathcal{Z}^m \subseteq \mathbb{R}^{md}$	Codomain of Z
θ_{Bayes}	Bayes estimator
$f^*(z) = \mathbb{E}(\theta Z = z)$	Bayes estimator as function of z
$p_{\theta, m}(z)$	Density of Z
$\phi_m = (w, \beta)$	Neural network parametrization with m input samples
L	Number of layers in neural network
$\{w^{(l)}\}_{l=1, \dots, L}$	Weight matrices of neural network
$\{\beta^{(l)}\}_{l=1, \dots, L}$	Bias vectors of neural network
ϕ_m^*	Optimal parametrization
f	A mapping, usually from \mathcal{Z}^m to Θ
f_ϕ	Map from \mathcal{Z}^m to Θ defined by ϕ
$\ell(x, y) = \ x - y\ _2^2$	Quadratic loss function
$R(f)$	Risk of f
$R_N(f)$	Empirical risk of f
$R(\phi)$	Risk of f_ϕ
$R_N(\phi)$	Empirical risk of f_ϕ
$R(f_m^*)$	Bayes Risk
ϕ_m^*	Optimal parametrization with respect to R
ϕ_m^N	Optimal parametrization with respect to R_N
$\tilde{\phi}_m^N$	Approximation of ϕ_m^N during training
t_m^ε	Test statistic for Bernstein–von Mises Theorem
B	Bound on parameter space Θ
$D = md$	Input dimension of neural network
M	Bound on input space of neural network, bound in uniform tightness condition
$\phi_m^{N, \alpha}$	Restricted empirical risk minimizer
$\mathcal{X} = \mathcal{Z}^m \subseteq \mathbb{R}^{md}$	Input space of neural network
$\mathcal{Y} \approx \Theta$	Output space of neural network
\mathcal{F}	Subset of functions $f : \mathcal{X} \rightarrow \mathcal{Y}$
$s = (x, y) \in (\mathcal{X} \times \mathcal{Y})$	Training sample (realization)
$S = (X, Y)$	Training sample (random variable)
$A_s \in \mathcal{F}$	Function output by algorithm A for sample s
E	Upper bound on loss function
K	Number of disjoint sets in robustness definition
$\varepsilon(s)$	Robustness parameter
δ	Probability of error bound

References

- J. Alsing, T. Charnock, S. Feeney, and B. Wandelt. Fast likelihood-free cosmology with neural density estimators and active learning. *Monthly Notices of the Royal Astronomical Society*, 488(3):4440–4458, 2019. doi: 10.1093/mnras/stz1960. URL <https://doi.org/10.1093/mnras/stz1960>.
- T. Anderson. *An Introduction to Multivariate Statistical Analysis, 3rd Ed.* Wiley India Pvt. Limited, 2003. ISBN 9788126524488. URL <https://books.google.ch/books?id=1iFOCgAAQBAJ>.
- M. A. Beaumont, W. Zhang, and D. J. Balding. Approximate bayesian computation in population genetics. *Genetics*, 162(4):2025–2035, 2002.
- F. Bokma. Artificial neural networks can learn to estimate extinction rates from molecular phylogenies. *Journal of Theoretical Biology*, 243(3):449–454, 2006.
- B. M. Brown and S. I. Resnick. Extreme values of independent stochastic processes. *J. Appl. Probab.*, 14:732–739, 1977.
- G. Buriticá and S. Engelke. Progression: an extrapolation principle for regression, 2024. URL <https://arxiv.org/abs/2410.23246>.
- K. H. Chon and R. J. Cohen. Linear and nonlinear arma model parameter estimation using an artificial neural network. *IEEE transactions on biomedical engineering*, 44(3):168–174, 1997.
- G. Cybenko. Approximation by superpositions of a sigmoidal function. *Mathematics of control, signals and systems*, 2(4):303–314, 1989.
- L. de Haan. A spectral representation for max-stable processes. *Ann. Probab.*, 12:1194–1204, 1984.
- C. Dombry, F. Éyi Minko, and M. Ribatet. Conditional simulation of max-stable processes. *Biometrika*, 100(1):111–124, 2012. doi: 10.1093/biomet/ass067. URL <https://doi.org/10.1093/biomet/ass067>.
- C. Dombry, S. Engelke, and M. Oesting. Exact simulation of max-stable processes. *Biometrika*, 103:303–317, 2016.
- C. Dombry, S. Engelke, and M. Oesting. Asymptotic properties of the maximum likelihood estimator for multivariate extreme value distributions, 2017a. URL <https://arxiv.org/abs/1612.05178>.
- C. Dombry, S. Engelke, and M. Oesting. Bayesian inference for multivariate extreme value distributions. *Electronic Journal of Statistics*, 11(2):4813 – 4844, 2017b. doi: 10.1214/17-EJS1367. URL <https://doi.org/10.1214/17-EJS1367>.
- S. Engelke and A. S. Hitz. Graphical models for extremes (with discussion). *J. R. Stat. Soc. Ser. B Stat. Methodol.*, 82(4):871–932, 2020. doi: <https://doi.org/10.1111/rssb.12355>. URL <https://rss.onlinelibrary.wiley.com/doi/abs/10.1111/rssb.12355>.
- F. Gerber and D. Nychka. Fast covariance parameter estimation of spatial gaussian process models using neural networks. *Stat*, 10(1):e382, 2021.
- I. Goodfellow, Y. Bengio, and A. Courville. *Deep Learning*. MIT Press, 2016. <http://www.deeplearningbook.org>.

- C. Gouieroux, A. Monfort, and E. Renault. Indirect inference. *Journal of Applied Econometrics*, 8(S1):S85–S118, 1993. doi: <https://doi.org/10.1002/jae.3950080507>. URL <https://onlinelibrary.wiley.com/doi/abs/10.1002/jae.3950080507>.
- E. J. Gumbel. Distributions des valeurs extrêmes en plusieurs dimensions. *Publ. Inst. Statist. Univ. Paris*, 9:171–173, 1960.
- M. Hentschel, S. Engelke, and J. Segers. Statistical inference for Hüsler–Reiss graphical models through matrix completions. *Journal of the American Statistical Association*, 0(0):1–13, 2024.
- J. Hüsler and R.-D. Reiss. Maxima of normal random vectors: Between independence and complete dependence. *Statist. Prob. Letters*, 7(4):283–286, February 1989. URL <https://ideas.repec.org/a/eee/stapro/v7y1989i4p283-286.html>.
- Y. Jiao, G. Shen, Y. Lin, and J. Huang. Deep nonparametric regression on approximate manifolds: Nonasymptotic error bounds with polynomial prefactors. *The Annals of Statistics*, 51(2):691 – 716, 2023. doi: 10.1214/23-AOS2266. URL <https://doi.org/10.1214/23-AOS2266>.
- Z. Kabluchko, M. Schlather, and L. de Haan. Stationary max-stable fields associated to negative definite functions. *The Annals of Probability*, 37(5):2042 – 2065, 2009. doi: 10.1214/09-AOP455. URL <https://doi.org/10.1214/09-AOP455>.
- E. LeDell and S. Poirier. H2O AutoML: Scalable automatic machine learning. *7th ICML Workshop on Automated Machine Learning (AutoML)*, July 2020. URL https://www.automl.org/wp-content/uploads/2020/07/AutoML_2020_paper_61.pdf.
- A. Lenzi, J. Bessac, J. Rudi, and M. L. Stein. Neural networks for parameter estimation in intractable models, 2021.
- T. Poggio, H. Mhaskar, L. Rosasco, B. Miranda, and Q. Liao. Why and when can deep-but not shallow-networks avoid the curse of dimensionality: a review. *International Journal of Automation and Computing*, 14(5):503–519, 2017.
- J. Rudi, J. Bessac, and A. Lenzi. Parameter estimation with dense and convolutional neural networks applied to the fitzhugh–nagumo ode. In J. Bruna, J. Hesthaven, and L. Zdeborova, editors, *Proceedings of the 2nd Mathematical and Scientific Machine Learning Conference*, volume 145 of *Proceedings of Machine Learning Research*, pages 781–808. PMLR, 16–19 Aug 2022.
- H. Rue and L. Held. *Gaussian Markov Random Fields: Theory and Applications*, volume 104 of *Monographs on Statistics and Applied Probability*. Chapman and Hall/CRC, Boca Raton, FL, 2005. ISBN 978-1-58488-432-3. URL <https://www.crcpress.com/Gaussian-Markov-Random-Fields-Theory-and-Applications/Rue-Held/p/book/9781584884323>.
- M. Sainsbury-Dale, A. Zammit-Mangion, and R. Huser. Likelihood-free parameter estimation with neural bayes estimators. *The American Statistician*, pages 1–23, 2023.
- J. Schmidt-Hieber. Nonparametric regression using deep neural networks with ReLU activation function. *The Annals of Statistics*, 48(4):1875 – 1897, 2020. doi: 10.1214/19-AOS1875. URL <https://doi.org/10.1214/19-AOS1875>.
- X. Shen and N. Meinshausen. Engression: Extrapolation through the lens of distributional regression, 2024. URL <https://arxiv.org/abs/2307.00835>.
- M. L. Stein. *Interpolation of spatial data: some theory for kriging*. Springer Science & Business Media, 2012.

- A. W. van der Vaart. *Asymptotic Statistics*. Cambridge Series in Statistical and Probabilistic Mathematics. Cambridge University Press, 1998. doi: 10.1017/CBO9780511802256.
- C. Varin, N. Reid, and D. Firth. An overview of composite likelihood methods. *Statistica Sinica*, 21(1):5–42, 2011. ISSN 10170405, 19968507. URL <http://www.jstor.org/stable/24309261>.
- J. L. Wadsworth. On the occurrence times of componentwise maxima and bias in likelihood inference for multivariate max-stable distributions. *Biometrika*, 102(3):705–711, 2015. URL <http://www.jstor.org/stable/43910215>.
- J. Walchessen, A. Lenzi, and M. Kuusela. Neural likelihood surfaces for spatial processes with computationally intensive or intractable likelihoods. *Spatial Statistics*, 62:100848, Aug. 2024. ISSN 2211-6753. doi: 10.1016/j.spasta.2024.100848. URL <http://dx.doi.org/10.1016/j.spasta.2024.100848>.
- C. Xing, D. Arpit, C. Tsirigotis, and Y. Bengio. A walk with sgd, 2018. URL <https://arxiv.org/abs/1802.08770>.
- H. Xu and S. Mannor. Robustness and generalization. *Machine learning*, 86:391–423, 2012.
- D. Yarotsky. Error bounds for approximations with deep relu networks. *Neural Networks*, 94:103–114, 2017.
- A. Zammit-Mangion, M. Sainsbury-Dale, and R. Huser. Neural methods for amortized inference. *Annual Review of Statistics and Its Application*, 12(Volume 12, 2025):311–335, 2025. doi: <https://doi.org/10.1146/annurev-statistics-112723-034123>.
- Z. Zhang, D. Bolin, S. Engelke, and R. Huser. Extremal dependence of moving average processes driven by exponential-tailed lévy noise, 2023. URL <https://arxiv.org/abs/2307.15796>.